Repeated mitochondrial capture with limited genomic introgression in a lizard group

Running title: mtDNA capture with limited nuDNA introgression

Authors: Wesley J. Read[1]*, Rebecca J. Laver[1,2], Ching Ching Lau[1], Craig Moritz[1], & Stephen M. Zozaya[1]

[1]Division of Ecology and Evolution, Research School of Biology, The Australian National University, Acton, Australian Capital Territory, Australia.
[2]The University of the Sunshine Coast, Moreton Bay Campus, Petrie, QLD, Australia.
*Corresponding author: wesley.read@anu.edu.au

Author contributions: WJR, SMZ, and CM conceived the study; WJR, CCL, and RJL performed bioinformatics procedures; WJR, SMZ, and CCL performed analyses; WJR and SMZ created figures; WJR drafted the manuscript; all authors contributed to editing the final manuscript.

Funding: This work was funded by Australian Research Council Discovery Projects DP190102395 and DP210102267, and an Australian Biological Resources Study NTRGP Postdoctoral Fellowship Grant to SMZ.

Data Accessibility Statement: All data and R code available at https://doi.org/10.6084/m9.figshare.28440584

Conflicts of interest: The authors declare no conflicts of interest.

Ethics approval statement: Newly acquired samples were collected under Australian National University animal ethics approvals A2019/15 and A2022/07, Western Australia Regulation 25 scientific purposes permit FO25000338-3, and NT Parks and Wildlife Commission permit number 69132.

Abstract

Mitochondrial introgression is common among animals and is often first identified through mitonuclear discordance — discrepancies between evolutionary relationships inferred from mitochondrial DNA (mtDNA) and nuclear DNA (nuDNA). Over recent decades, genomic data have also revealed extensive nuclear introgression in many animal groups, with implications for genetic and phenotypic diversity. However, the extent to which mtDNA introgression corresponds to nuDNA introgression varies. Here, we investigated historical and recent introgression in the *Gehyra nana-occidentalis* clade, a complex group of Australian geckos with documented cases of mitonuclear discordance suggestive of repeated mtDNA introgression. We hypothesised that mitonuclear discordance in this clade reflects mtDNA introgression with substantial nuclear introgression. Despite evidence of repeated mtDNA introgression, however, we found little to no evidence of historical nuDNA introgression using exon capture and genome-wide single nucleotide polymorphism (SNP) data. We also found no evidence of gene flow at modern contact zones and detected only a single early generation hybrid. Unsurprisingly given these results, we found no evidence of transgressive, intermediate, or more variable morphological phenotypes in taxa with introgressed mtDNA. These findings suggest that hybridisation in this system has, at least in some cases, resulted in repeated mitochondrial introgression with little or no nuclear introgression. This pattern aligns with other studies showing limited nuDNA introgression in taxa with mitonuclear discordance, highlighting a potentially broader trend in animal radiations.

Keywords: mitonuclear discordance, contact zone, hybridisation, exon capture, SNP, *Gehyra*

Introduction

Hybridisation was once thought to occur rarely in animals (Mayr, 1963), but modern phylogenomics has revealed extensive, post-divergence gene flow across many taxa (Abbott et al., 2013; Mallet et al., 2016). One potential outcome of hybridisation is the exchange of mitochondria between lineages, whereby 'lineage' can refer to a genetic lineage within a species or a species itself. This is known as mitochondrial introgression, which is now recognised as common across many taxa (Currat et al., 2008; Toews & Brelsford, 2012). However, the extent to which matching nuclear introgression occurs can vary from extensive (e.g., Sarver et al., 2021; Ji et al., 2023) to limited or absent (e.g., Sloan et al., 2017; Grummer et al., 2018; Mao & Rossiter, 2020). Mitonuclear discordance — where evolutionary relationships inferred from mtDNA differ to those inferred from nuDNA — is often the first indication of mtDNA introgression (e.g., Phuong & Moritz, 2017; Pavón-Vásquez et al., 2024). In some cases, mitonuclear discordance may also

indicate a homoploid hybrid species, which form instantly via hybridisation; but these appear exceptionally rare (Schumer et al., 2014; Hill, 2019). Species groups showing mitonuclear discordance offer valuable opportunities to examine levels of accompanying nuclear gene flow.

Introgression can have significant consequences for lineage divergence and phenotypic variation. If introgression is too frequent it can swamp the genome, potentially reversing the speciation process (Rhymer & Simberloff, 1996; Todesco et al., 2016). Alternatively, introgression may trigger or facilitate speciation (Edelman & Mallet, 2021) by, for example, introducing adaptive variation (e.g., Staubach et al., 2012) or by altering phenotypes (Lamichhaney et al., 2015; Taylor & Larson, 2019 and references therein). Introgressed populations may exhibit novel (transgressive) phenotypes through epistatic interactions or novel allelic combinations (Dittrich-Reed & Fitzpatrick, 2013), or intermediate or more variable phenotypes driven by epistasis or heterozygosity for genes with incomplete dominance (Masello et al., 2019). Transgressive phenotypes are of particular interest in adaptive radiations as access to novel trait space may allow expansion into new niches, thereby facilitating rapid diversification (Pfennig et al., 2016; Wogan et al., 2023). Introgression, therefore, treads a fine line between promoting and inhibiting divergence and, thus, has important implications for understanding diversification (Cruickshank & Hahn, 2014; Harrison & Larson, 2014) and species boundaries (Hillis et al., 2021; Barley et al., 2024).

As the mitochondrial genome is effectively a single, non-recombining gene, mitonuclear discordance might not correspond to matching nuDNA introgression. So called ‘massive discordance’ may occur when a species' native mitochondrial genome is nearly or entirely replaced by mtDNA introgression without matching nuclear introgression (Bonnet et al., 2017). However, determining whether there has been mtDNA introgression based on contrasting mtDNA and nuDNA phylogenies is not straightforward; one must also consider incomplete lineage sorting (ILS) and tree estimation error (Larson et al., 2024). Indeed, identifying introgression in general — whether mtDNA or nuDNA — can be complicated by ILS and the loss of phylogenetic signal through time (Galtier & Daubin, 2008). Model parameter misspecification (Cooper, 2014; Huang et al., 2022) and failure to consider selection (Smith & Hahn, 2024) can also mislead introgression estimates. Establishing confidence in introgression estimates therefore relies on comparing results across different methods of analysis (Hibbins & Hahn, 2022).

We explored whether mitonuclear discordance correspond to genomic introgression in a clade of *Gehyra* geckos from the Kimberley region of northern Australia. *Gehyra* is a genus of morphologically conservative geckos with a broad distribution across Australia, Wallacea, Melanesia, and south-east Asia (Heinicke et al., 2011). *Gehyra* diversity is highest in Australia,

with 50 recognised species (Wilson & Swan, 2020; Uetz et al., 2024) comprising two broad clades of Plio-Miocene origin: the typically small-bodied *punctata-variegata* group (Ashman et al., 2018), and the large-bodied *australis* group (Sistrom et al., 2009; Oliver et al., 2020). Several unresolved species complexes remain within the *punctata-variegata* group, including the *Gehyra nana* and *G. occidentalis* complexes of the Kimberley region (Oliver et al., 2016; Doughty et al., 2018; Lau et al., 2025), which we hereafter refer to as the *nana-occidentalis* clade. Phylogenetic analyses of the *nana-occidentalis* clade, using geographically dense sampling of mtDNA and exon capture sequencing, have identified eight lineages within this group (Figure 1; Oliver et al., 2016; Moritz et al., 2018; Lau et al., 2025): *nana*1, *nana*2, *nana*4, and nanamulti in the *G. nana* complex; *occidentalis*-KL, *occidentalis*-OR, *occidentalis*-YI, and *G. multiporosa* (simply '*multiporosa*' hereafter) in the *G. occidentalis* complex. Lineages within each of the two complexes are morphologically similar and typically replace each other at parapatric boundaries, although *nana*4 and nanamulti occur in mosaic sympatry. In contrast, members of the smaller-bodied *nana* complex often co-occur with members of the *occidentalis* complex. Of particular interest in this clade is the strong evidence of mitonuclear discordance. One example is the nanamulti lineage that — while nested within the *nana* complex for nuDNA — has mtDNA that is interdigitated within *multiporosa* (Moritz et al., 2018; Figure 1), suggesting repeated mtDNA introgression between these distantly-related lineages, rather than simple estimation error or ILS. The sympatry with nana4 and massive introgression for mtDNA suggests the hypothesis that nanamulti itself possibly arose via homoploid hybrid speciation. Further mitonuclear discordance is observed among lineages in the *occidentalis* complex (Figure 1; Oliver et al., 2016; Moritz et al., 2018; Lau et al., 2025), although here evidence of mtDNA introgression, rather than ILS, is less clear as each lineage is reciprocally monophyletic and phylogenetically within the same species complex (unlike nanamulti and *multiporosa*). Given such complex mitonuclear discordance, this group offers a good opportunity to investigate whether mitonuclear discordance corresponds to substantial nuclear introgression.

Here, we used exon capture and genome-wide SNP data to test for both historical and recent genomic introgression in the *nana-occidentalis* clade. We first performed hypothesis-based tests of historical introgression informed by cases of mitonuclear discordance, the results of which we then corroborated using D-statistics. We then assessed recent or ongoing introgression at two modern contact zones that include lineages with evidence of mitonuclear discordance. Finally, we assessed whether lineages with introgressed mtDNA exhibit transgressive, intermediate, or more variable phenotypes.

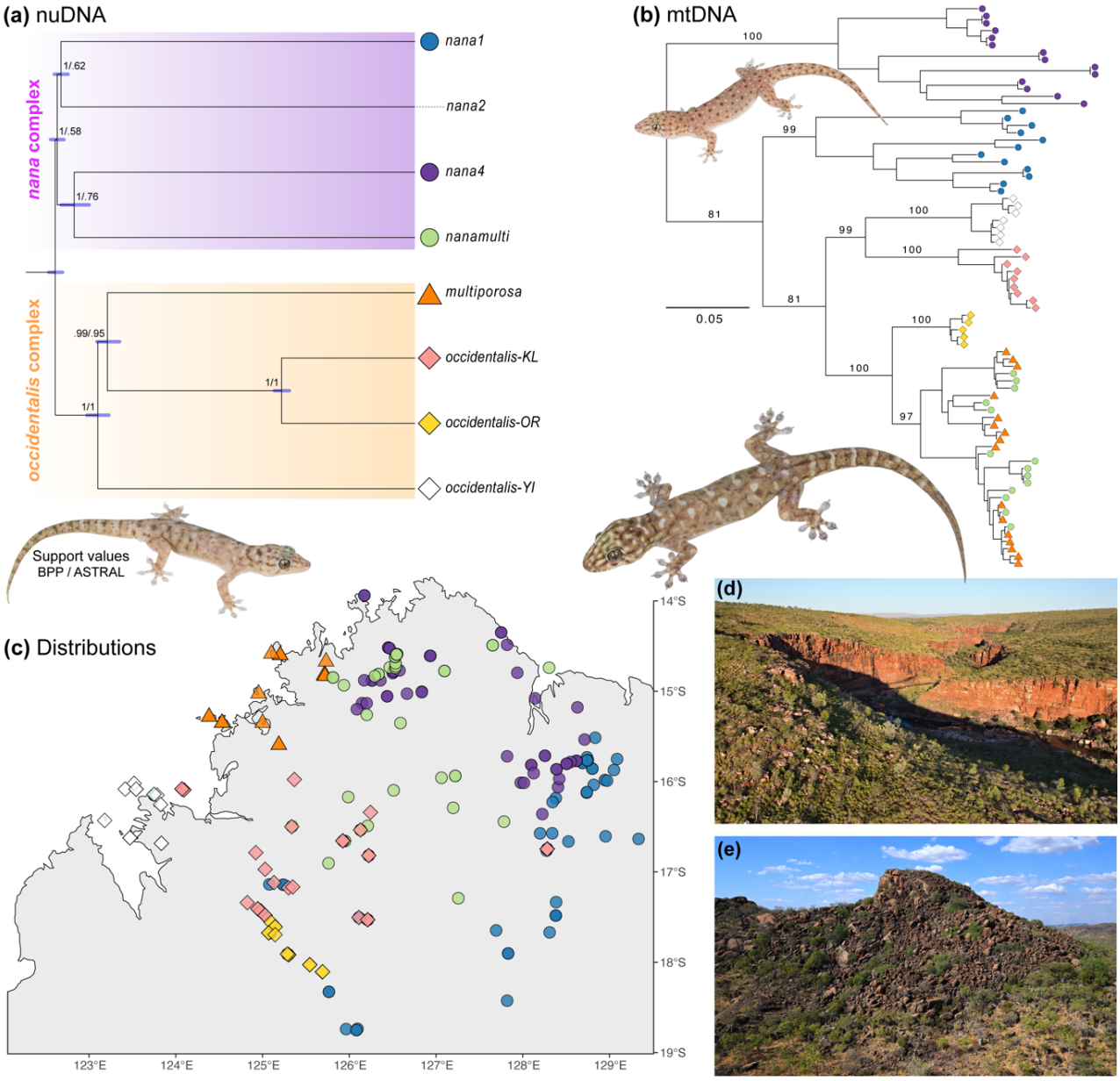

FIGURE 1. Relationships and distributions of the *Gehyra nana-occidentalis* clade. (a) Species tree inferred from 1000 nuDNA exons using BPP, with support shown for both BPP and ASTRAL (identical topologies). Note that *nana*2 is included here but not elsewhere as it occurs outside the focal Kimberley region. (b) MtDNA relationships among focal lineages inferred with IQ-TREE, showing several cases of discordance with respect to nuDNA ancestry. Ultrafast bootstrap support values are shown for major branches. (c) Lineage distributions in Australia's Kimberley region based on samples with nuDNA data. (d–e) Typical habitat, showing sandstone gorges (d) and granite boulders (e). Gecko photos show *occidentalis*-OR (left), *nana*4 (top-right), and *occidentalis*-KL (bottom-right). Photos: Ian Bool (d,e); Scott Macor (geckos).

Methods

Exon capture sequence data

We obtained published nuDNA exon capture sequence data spanning > 1,000 loci to perform phylogenetic network analyses. Sequence data were acquired from Moritz et al. (2018) and Lau et al. (2025) for the following *Gehyra* species/lineages: *nana*1, *nana*2, *nana*4, nanamulti, *multiporosa*, *occidentalis*-KL, *occidentalis*-OR, and *occidentalis*-YI, with *G. paranana* used as the outgroup. These included 67 samples with 4–14 samples per focal lineage and a single sample of *G. paranana* (Table S1). Briefly, these data were produced using the exon capture approach described in Moritz et al. (2018), which targeted approximately 1900 single-copy exons. Sequences were processed, filtered, and aligned using the EAPhy pipeline (Blom, 2015). Loci with ≥ 11 missing individuals (i.e., ≥ 15% missing data) were removed to maximise individual coverage while retaining ≥ 1000 loci. We then removed six individuals with ≥ 40% missing data, and another two samples with uncertain locality data, retaining 58 samples for subsequent analysis (see Table S1). The final dataset comprised 1,478 exonic loci, ranging from 108–2,088 bp in length (mean = 334 bp; median = 228 bp), totalling 494,507 bp across all loci, with 20,517 parsimony-informative and 21,166 singleton sites. Alignments were manually inspected prior to subsequent analysis to ensure correct reading frames, with no missense mutations or unexpected stop codons within the respective exons.

SNP data

Genome-wide reduced-representation sequencing was done to obtain genome-scale SNP data to test historical introgression using *D*-statistics and to perform contact zone analyses. Contact zones were identified based on previously published data (Moritz et al., 2018; Doughty et al., 2018; Fenker et al., 2021; Lau et al., 2025). We used DArTseq via Diversity Arrays Technology (DArT; Canberra, Australia), which involves genome fragmentation with two restriction enzymes (PstI/HpaII) followed by filtering based on fragment size and subsequent Illumina short-read sequencing (Sansaloni et al., 2010; Kilian et al., 2012), yielding thousands of 60–80 bp sequence fragments. SNP calling and associated filtering is then done across all samples via DArT's proprietary pipeline. Newly generated DArTseq data (n = 35) were combined with data for relevant lineages from Fenker et al. (2021) and Lau et al. (2025). Our final dataset included 242 individuals sampled across lineage ranges and contact zones, and including *G. paranana* as an outgroup (Table S2). DNA was extracted for newly sequenced samples using a Qiagen DNeasy Blood & Tissue Kit.

SNP data were filtered separately for each analysis to maximise the number of variant sites for each data subset. We used dartR v.2.9.7 (Gruber et al., 2018) to filter data in the following order: minimum read depth ≥ 6; maximum read depth ≤ 80 (resulting in no losses); reproducibility ≥ 0.99; call rate by locus ≥ 0.8; call rate by individual ≥ 0.5; minor allele count ≥ 3 (to ensure a given allele is present in at least two individuals); removal of monomorphic loci; retain only one variant site per locus (using method = "best" to retain the site with the highest PIC score). The final dataset of samples across all focal lineages contained 3,966 variant sites. Before continuing, we used the *gl.pcoa()* function in dartR to perform a Principal Coordinates Analysis (PCoA) on these data to confirm the lineage assignment of newly sequenced samples (Figure S1). After filtering, a total of 1,828 variant sites were retained for the *multiporosa*/nanamulti contact zone, and 2,192 variant sites were retained for the nanamulti/nana4 contact zone.

mtDNA data and phylogenetics

Phylogenetic analysis of mtDNA sequence data was done to illustrate the mitonuclear discordance demonstrated in previous studies. For relevant lineages, we obtained sequence data for the 1,038 bp *NADH dehydrogenase subunit 2 (ND2)* locus from previous studies (Doughty et al., 2012; Oliver et al., 2017; Moritz et al., 2018; n = 468). We then generated new *ND2* sequences for those samples with genomic data but lacking mtDNA data (n = 132) using the MinION barcoding method from Srivathsan et al. (2021). Methods followed those presented in Zozaya et al. (2024) except using the primers M112F (5'- AAGCTTTCGGGGCCCATACC -3') and M1123R (5'- GCTTAATTAAAGTGTYTGAGTTGC -3') from Sistrom et al. (2009). The resulting *ND2* sequences were aligned with those obtained from previous studies using MAFFT in Geneious Prime v. 2021.2.2, which yielded a final alignment of 1,038 bp across 600 samples, including one *G. spheniscus* as the outgroup (Moritz et al., 2018). The alignment was inspected for gaps, unexpected stop codons, or frame shifts, followed by phylogenetic analysis using IQ-TREE v. 2.2.0 (Minh et al., 2020). The alignment was partitioned by codon position, with ModelFinder (Kalyaanamoorthy et al., 2017) used to determine the best partition scheme and substitution model, and statistical support determined with 1000 ultrafast bootstrap (UFB) replicates (Hoang et al., 2018). The final partition and model scheme was: 1st position (TIM+F+I+G4); 2nd position (TVM+F+G4); 3rd position (GTR+F+I+G4). We also re-ran this analysis with a subset of 78 samples—chosen to represent mtDNA diversity in each lineage—to better visualise mtDNA relationships with fewer samples.

NuDNA phylogenomics

Our analyses of historical introgression depend on accurate knowledge of phylogenetic relationships. Given the varying phylogenetic relationships inferred for the *nana-occidentalis* clade, including variable support for the monophyly of lineages of *G. nana* itself in previous studies (Moritz et al., 2018; Ashman et al., 2018; Lau et al., 2025), we performed several phylogenomic analyses using exon capture sequence data to better understand relationships among the *nana-occidentalis* clade. Although it occurs outside our study area, we included the Northern Territory *nana*2 lineage in all phylogenomic analyses to test the monophyly of *G. nana*. All phylogenomic analyses used the exon capture dataset. We first performed maximum likelihood (ML) phylogenetic analysis on the concatenated 1,478 exon alignment using IQ-TREE v2.2.2.6 (Minh et al., 2020) to confirm lineage assignment for all samples. The analysis was partitioned by locus with modelfinder (Lanfear et al., 2012; Kalyaanamoorthy et al., 2017) used to determine the best partition scheme (MFP+merge) and substitution models. We specified 1000 UFB replicates implemented via ufboot2 (Hoang et al., 2018) in addition to branch support metrics via a Shimodaira–Hasegawa-like approximate likelihood ratio test (SH-aLRT; Guindon et al., 2010; Hoang et al., 2018) with 1000 replicates. We used genesite resampling to resample partitions and sites within partitions (Gadagkar et al., 2005; Seo et al., 2005). Next, we performed species tree analysis using the quartet-based algorithm implemented in ASTRAL-III v5.7.8 (Rabiee et al., 2019). ASTRAL requires gene trees as input, which were estimated for each of the 1,478 exons using IQ-TREE v2.2.2.6, with modelfinder used to determine the best substitution model for each locus, with 1000 UFB replicates. Prior to ASTRAL analysis, gene tree branches with bootstrap support < 30 were collapsed using TreeCollapserCL4 (Hodcroft, 2016) to improve species tree accuracy and branch support (Simmons & Gatesy, 2021). Finally, we used BPP v4.7 (Flouri et al., 2018) to perform Bayesian multispecies coalescent phylogenetic analysis. We used the 1,000 longest exons (180–2,088 bp; mean = 418 bp; median = 333 bp) with a maximum of seven missing individuals, using 3–4 individuals with the least missing data from each lineage, and with one *G. paranana* sample included as an outgroup (Table S1). The analysis was initially run as an A01, specifying the guide tree topology as inferred by ASTRAL-III. We assigned diffuse inverse-gamma priors for population size $\theta \sim$ InvGamma(3, 0.003) and tree height $\tau \sim$ InvGamma(3, 0.003). Units for both θ and τ represent the expected number of mutations per site. We ran the MCMC for 1,000,000 iterations after a burn-in of 100,000 iterations, with sampling every two iterations for a total of 500,000 samples.

Testing historical introgression using network analysis

We conducted hypothesis-based tests of introgression using the multi-species-coalescence-with-introgression (MSCi) phylogenetic network analysis in BPP v.4.4.0 (Flouri et al., 2020) to specifically test for genomic introgression in cases where there is evidence of mitonuclear discordance (Figure 1). Specifically, we tested for introgression between: i) *multiporosa* and nanamulti; ii) *multiporosa* and *occidentalis*-OR; and iii) *occidentalis*-YI and *occidentalis*-KL. There is clear evidence of repeated mtDNA introgression from *multiporosa* to nanamulti, whereas there are two equivocal scenarios of mtDNA introgression within the *occidentalis* complex (see Results). BPP makes full use of the sequence data under the MSC, produces robust inferences even under model miss-specification (Huang et al., 2022), and is computationally efficient. Analyses used subsets of the same 1,000 loci used for the phylogenomic analysis above. As BPP requires a user-specified phylogeny, analyses were run with three tips to avoid the uncertain phylogenetic relationships and reduce computational burden. Three tips were used, rather than two, because the MSCi cannot estimate introgression when the lineages involved are sisters (Hibbins & Hahn, 2022). The following relationships were specified for each combination of lineages: i) (*multiporosa*, (nanamulti, *nana*4)); ii) (*multiporosa*, (*occidentalis*-OR, *occidentalis*-KL)); iii) (*occidentalis*-YI, (*occidentalis*-KL, *occidentalis*-OR)). Each tip included 3–4 of the most data complete samples (Table S1). Three introgression scenarios — two unidirectional models and one bidirectional model — were run for each of these lineage combinations. For example, unidirectional introgression was tested from *multiporosa* to nanamulti and then from nanamulti to *multiporosa*, each as a separate analysis, and then a model was run with bidirectional introgression between the two lineages. Priors for population size (θ) and tree height (τ) were both assigned as InvGamma(3, 0.003), while the prior for introgression probability (φ) was assigned as Beta(2, 4). Values for φ represent the proportion of the genome that traces its ancestry via the introgression edge (Flouri et al., 2020). Each analysis was run for 1,000,000 iterations after a burn-in of 100,000 iterations, sampling every two iterations, for a total of 500,000 sampled iterations. All analyses were executed twice to check for convergent results, and posterior distributions were checked using TRACER v.1.7.2 (Rambaut et al., 2018). We assessed the statistical significance for each model by calculating Bayes factors (B_{10}) via the Savage-Dickey density ratio (Dickey, 1971), which uses the MCMC sample to assess whether the posterior distribution of φ differs from what would be expected given the priors, with $B_{10} \geq 20$ indicating a strongly supported introgression event (Ji et al., 2023).

Tests for historical introgression using D-statistics

We used the genome-wide SNP dataset to estimate *D*- and f-branch statistics using *Dsuite* (Malinsky et al., 2021). This method assesses all lineage combinations for introgression, except sister lineages, and then accounts for correlated allele frequencies among tips to identify introgression events on the internal branches of the tree (Durand et al., 2011; Patterson et al., 2012). We specified the topology recovered by both ASTRAL and BPP, again using *G. paranana* as the outgroup. P-values were calculated using the jack-knife method and, as more than three lineages were assessed, we applied the False Discovery Rate (FDR) correction to account for false positives due to multiple pairwise comparisons (Benjamini & Hochberg, 1995) using the 'p.adjust' function as suggested by Malinsky et al. (2021).

Contact zone analyses

We analysed two contact zones, one between *multiporosa* and nanamulti, and another between *nana*4 and nanamulti. All analyses described below were run separately for each of these two contact zones, and SNP filtering (see above) was done separately for each to maximise the number of variant sites. We first used NewHybrids (Anderson & Thompson, 2002) to test whether any individuals were F1, F2, or first-generation backcross (BC1) hybrids. This was done with the SNP dataset via the *gl.nhybrids()* in dartR using the 'AvgPIC' method, 100 sweeps, and a burn-in of 100. Next, we estimated the optimal number of ancestral populations (K) and individual admixture proportions using sNMF (Frichot et al., 2014) via the R package *LEA* (Frichot & Rançois, 2015). Genotypic clustering analyses can under- or over-estimate the optimal K value, and thus admixture estimates, when there is strong population structure and sparse or uneven sampling (Puechmaille, 2016; Lawson et al., 2018; Wang, 2022). To mitigate the influence of within-lineage population structure, we excluded samples outside a 40–80 km radius (depending on the lineages included and sampling density; Table S3) centred on each contact zone. Each analysis was run with K = 1–5, alpha = 100, 100 repetitions, and masking = 0.05. We considered the optimal K value to be the one that produced the lowest average cross entropy (ce) score. Given the biases mentioned above, we verified both the K and admixture estimates using isolation-by-distance (IBD) plots (e.g., Prates et al., 2023; Zozaya et al., 2024), which plot pairwise geographic distance against genome-wide average pairwise F_{ST} (Wright, 1943; Weir & Cockerham,1984; Weir & Hill, 2002) among individuals at each contact zone. Pairwise geographic distances (km) were calculated using the *earth.dist()* function in *fossil* v0.4.0 (Vavrek, 2011) and pairwise F_{ST} was calculated using the *calculate.all.pairwise.fst()* function in *BEDASSLE* v1.6.1 (Bradburd et al., 2013). If there is no introgression at a given contact zone we expect between-lineage pairwise F_{ST} to be relatively high and unrelated to the geographic distances among samples, whereas if there

is recent or ongoing introgression we expect between-lineage pairwise F_{ST} to decrease as geographic distances decrease. Finally, for each contact zone we performed a PCoA using the *gl.pcoa()* function in dartR to further verify the optimal K value and visualise the major axes of genetic variation.

Morphometric analyses

Morphological data for relevant lineages were collected from adult genotyped specimens at the Western Australian Museum (WAM; Table S4). We measured 10 standardly used and ecologically relevant linear traits (Oliver et al., 2019; traits are illustrated in Figure S2) to the nearest 0.1 mm using Mitutoyo digital callipers: snout-to-vent length (SVL); head length (HL); snout length (SL); head width (HW); head depth (HD); orbit width (OR); width-between-eyes (WBE); inter-limb-length (ILL); hindlimb-length (HLL); and forelimb-length (FLL). Sample sizes for each lineage are: *multiporosa* = 15 (7 ♂, 8 ♀); *occidentalis*-KL = 45 (17 ♂, 28 ♀); *occidentalis*-YI = 13 (5 ♂, 8 ♀); *occidentalis*-OR = 5 (1 ♂, 4 ♀); nanamulti = 37 (17 ♂, 20 ♀); *nana*4 = 42 (21 ♂, 21 ♀); *nana*1 = 22 (11 ♂, 11 ♀).

Using these data, we first tested for sexual dimorphism via a permutational multivariate analysis of variance (PerMANOVA) using the R package *RRPP* (Collyer et al., 2015). Sexual dimorphism was tested using three lineages for which we had the largest sample sizes (*occidentalis*-KL, n = 45; *nana*1, n = 22; and *nana*4, n = 42). All traits were log transformed prior to analysis. We used the *lm.rrpp()* function with the 10 log-transformed morphological traits as dependent variables and lineage, sex, and their interaction as predictor variables with 10,000 permutations and as a type III MANOVA for significance testing. Consistent with other studies of *Gehyra* (Ashman et al., 2018), the effect of sex was not significant (df = 1/103, F = 2.976, Z = 1.532, R^2 = 0.006, P = 0.064; Table S5) and, therefore, was not considered in subsequent analyses. We then tested for morphological divergence among lineages. A PerMANOVA was performed using the 10 log-transformed traits as dependent variables with lineage as the predictor variable and 10,000 permutations for significance testing. We then ran pairwise contrasts using the *pairwise()* function for each lineage pair, followed by P-value adjustment using the *p.adjust()* function to account for inflated type 1 error with the FDR method (Benjamini & Hochberg, 1995). We visualised morphological variation and divergence, and identified traits associated with the greatest axes of variation, via a Principal Components Analysis (PCA) using the *rda()* function (scale = T) in the R package *vegan* (Dixon, 2003). Finally, we tested whether intraspecific phenotypic variation differed among lineages, which could reflect increased genetic variation due to introgression. We conducted a Fligner-Killeen test (Fligner & Killeen, 1976), a

non-parametric test that compares variances among multiple groups, even when the assumption of normality is violated, in this case by potential outliers of exceptionally large or small size. This is a univariate test and, as previous studies have established body size as the primary trait of variance in *Gehyra* (Sistrom et al., 2012; Ashman et al. 2018; Moritz et al., 2018), we assessed phenotypic variance using log-transformed SVL as a proxy for body size across all lineages.

Results

NuDNA phylogenomics

All eight previously identified lineages were each recovered as monophyletic clades with strong support (IQ-TREE: UFB = 100; ASTRAL: posterior probability (pp) ≥ 0.99 for all; Figures S3, S4). All three phylogenomic analyses recovered the *occidentalis* complex as a monophyletic clade with full support (Figures 1a, S3, S4), with *occidentalis*-YI being the deepest branching lineage, followed by *multiporosa*, and *occidentalis*-KL and *occidentalis*-OR as sister lineages. Relationships among the four lineages of the *nana* complex, however, differed between the concatenated and species tree approaches (Figures 1a, S3, S4). The concatenated IQ-TREE analysis placed *nana*4 as sister to the remaining *nana-occidentalis* clade (UFB = 97, aLRT = 98.3), reducing the "*nana* complex" to a modestly supported clade (UFB = 87, aLRT = 75.2) with *nana*2 recovered as the first-branching lineage and *nana*1 and nanamulti as sister lineages (UFB = 89, aLRT = 91.6). In contrast, the *nana* group was recovered as monophyletic with low support in the ASTRAL analysis (pp = 0.58) and high support in the BPP (pp = 1) analysis. Both species tree analyses recovered *nana*4 + nanamulti and *nana*2 + *nana*1 as sister pairs, although ASTRAL inferred this with low support (pp = 0.76 for *nana*4 + nanamulti; pp = 0.62 for *nana*2 + *nana*1) compared to BPP (pp = 1 for both sister pairs). With respect to the *nana* complex (nana1, nana2, *nana*4, and nanamulti), all relationships are consistent with the 100-locus StarBEAST2 phylogeny from Moritz et al. (2018). Notably, low support for relationships within the *nana* complex are associated with very short internode lengths in the species tree analyses. What is important for our introgression analyses below — which require phylogenetic relationships to be pre-specified — is that the species tree methods each recover *nana*4 and nanamulti as sister lineages.

MtDNA phylogenetics

Five of the seven focal lineages are recovered as monophyletic mtDNA clades (Figures 1b, S5), while individuals of nanamulti are extensively interdigitated among *multiporosa*, often with very short branch lengths between samples of different nuDNA ancestry. All individuals assigned to nanamulti by nuDNA SNP analyses (Figure S1) have *multiporosa* mtDNA and are distributed

across multiple, well-supported mtDNA clades within *multiporosa*. From these observations, we infer recent and repeated mtDNA introgression from *multiporosa* to nanamulti. *Gehyra occidentalis*-OR is recovered as sister to *multiporosa*/nanamulti with respect to mtDNA, despite *occidentalis*-OR having a close sister relationship with *occidentalis*-KL based on nuDNA. Furthermore, *occidentalis*-KL and *occidentalis*-YI are most closely related with respect to mtDNA despite *occidentalis*-YI being the first-branching lineage in the nuDNA phylogenies. These results suggest two possible cases of historical mtDNA introgression in the *occidentalis* complex – either from *occidentalis*-YI to *occidentalis*-KL resulting in their mtDNA clades being most closely related, or from *multiporosa* to *occidentalis*-OR leading to close relationships of their mtDNA lineages.

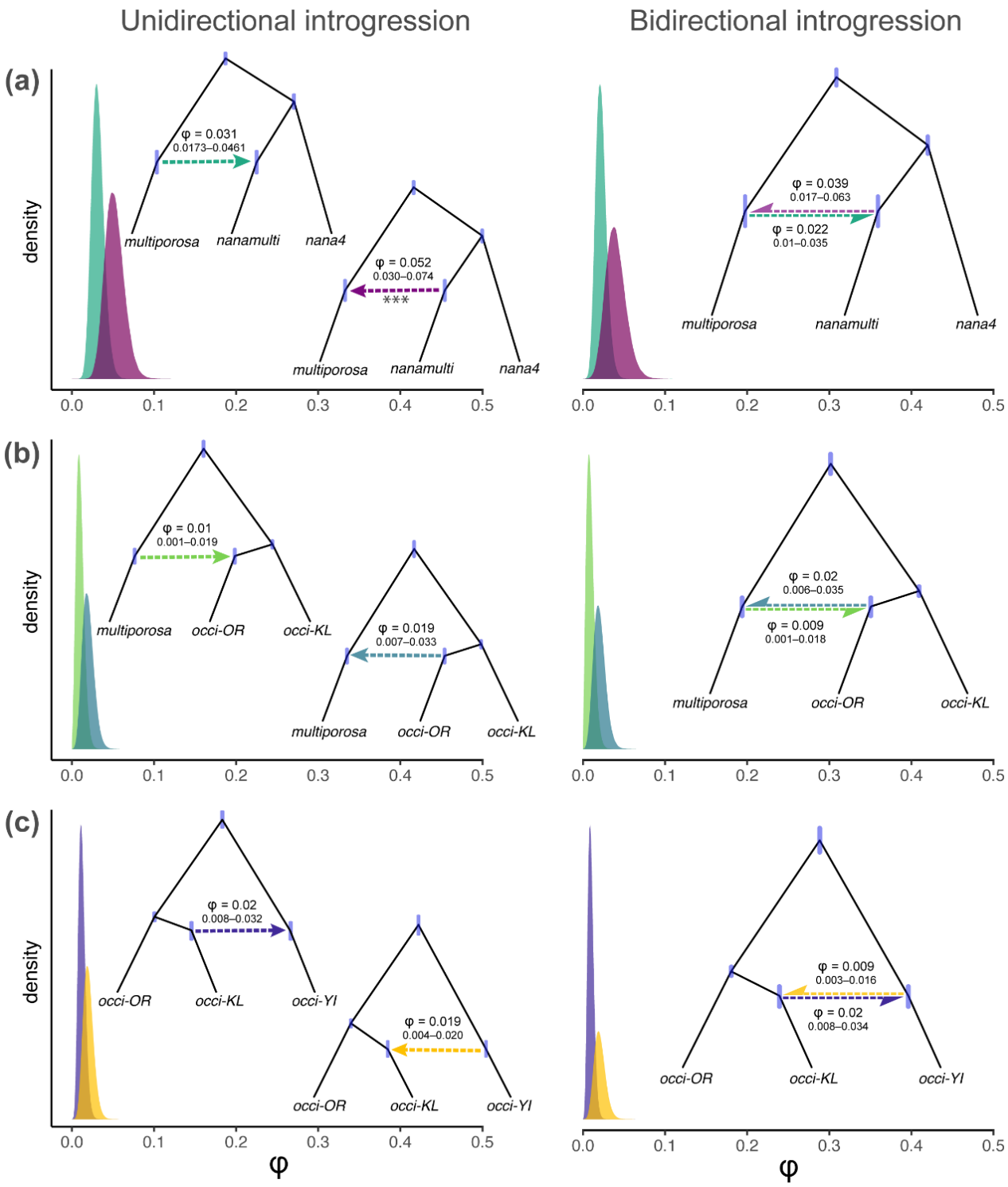

Figure 2. Results of hypothesis-based tests of introgression using the MSCi model implemented in BPP. Each row (a–c) shows a different combination of lineages. The left column shows results for unidirectional models; the right column shows results for the corresponding bidirectional model. Trees within panels show the scenarios being tested, with coloured arrows matching the posterior distributions within the respective panel. Values show means and 95% credible intervals for introgression probability (φ), which reflects the proportion of the genome that traces its ancestry via the introgression edge. Only the unidirectional model from nanamulti to *multiporosa* (***) was strongly supported ($B_{10} \geq 20$; Table 1).

Historical introgression

We used the MSCi in BPP to test introgression scenarios between *multiporosa* and nanamulti, *multiporosa* and *occidentalis*-OR, and *occidentalis*-YI and *occidentalis*-KL. Introgression was strongly supported ($B_{10} \geq 20$) only for unidirectional introgression from nanamulti to *multiporosa* ($\varphi = 0.0518$, 95% CI = 0.030–0.074; Figure 2; Table 1). This estimate of ~5.18% nuDNA introgression is low and in the opposite direction to what we expected given evidence of repeated mtDNA introgression from *multiporosa* to nanamulti. The unidirectional model from *multiporosa* to nanamulti received only modest support ($B_{10} = 12.26$) with lower introgression estimates (φ = 0.031, 95% CI = 0.017–0.046). All other introgression scenarios were poorly supported ($B_{10} < 1$).

In contrast to the MSCi results, estimates of excess allele sharing using the ABBA-BABA approach via *Dsuite* found no support for introgression between nanamulti and *multiporosa* (Figure 3). Excess allele sharing was inferred between the *nana*1 branch and each of the three *occidentalis* lineages, with estimates of up to 7% excess allele sharing. However, following recommendations by Malinsky et al. (2021) to implement FDR P-value adjustment and using $P < 0.01$ as the threshold for statistical significance, no excess allele sharing scenarios were supported as statistically significant ($P = 0.017–0.804$; Table S6).

Table 1. Results of MSCi phylogenetic network analysis using BPP. The 'Model' column shows whether the respective analysis tested unidirectional introgression (UDI) or bidirectional introgression (BDI). Values are the posterior means and 95% credible intervals (in parentheses) for introgression probability (φ, proportion of the genome that traces its ancestry via the introgression edge) and introgression time (τ, as the expected number of mutations per site), followed by Bayes factor (B_{10}) support. $B_{10} = \infty$ occurs if all φ values in the MCMC exceed the region of null effects (see Ji et al. 2023).

Model	Donor	Recipient	φ	$\tau(10^{-3})$	B_{10}
UDI	*multiporosa*	*nanamulti*	0.0315 (0.0173–0.0461)	1.255 (1.032–1.468)	12.26
UDI	*nanamulti*	*multiporosa*	0.0518 (0.0304–0.0746)	1.287 (1.092–1.499)	∞
BDI	*multiporosa*	*nanamulti*	0.0219 (0.0098–0.0349)	1.387 (1.157–1.606)	0.90
BDI	*nanamulti*	*multiporosa*	0.0397 (0.0171–0.0636)	1.387 (1.157–1.606)	0.06
UDI	*multiporosa*	*occidentalis-OR*	0.0099 (0.0015–0.0189)	0.861 (0.746–0.971)	0.00
UDI	*occidentalis-OR*	*multiporosa*	0.0198 (0.0069–0.0334)	0.896 (0.786–0.996)	0.01
BDI	*multiporosa*	*occidentalis-OR*	0.0089 (0.0009–0.018)	0.915 (0.814–1.01)	0.01
BDI	*occidentalis-OR*	*multiporosa*	0.0204 (0.006–0.035)	0.915 (0.814–1.01)	0.00
UDI	*occidentalis-YI*	*occidentalis-KL*	0.0197 (0.0043–0.0201)	0.8 (0.668–0.922)	0.00
UDI	*occidentalis-KL*	*occidentalis-YI*	0.02 (0.00816–0.0321)	0.652 (0.533–0.774)	0.02
BDI	*occidentalis-YI*	*occidentalis-KL*	0.0095 (0.003–0.0165)	0.742 (0.607–0.864)	0.02

BDI	*occidentalis-KL*	*occidentalis-YI*	0.0204 (0.0079–0.0339)	0.742 (0.607–0.864)	0.00

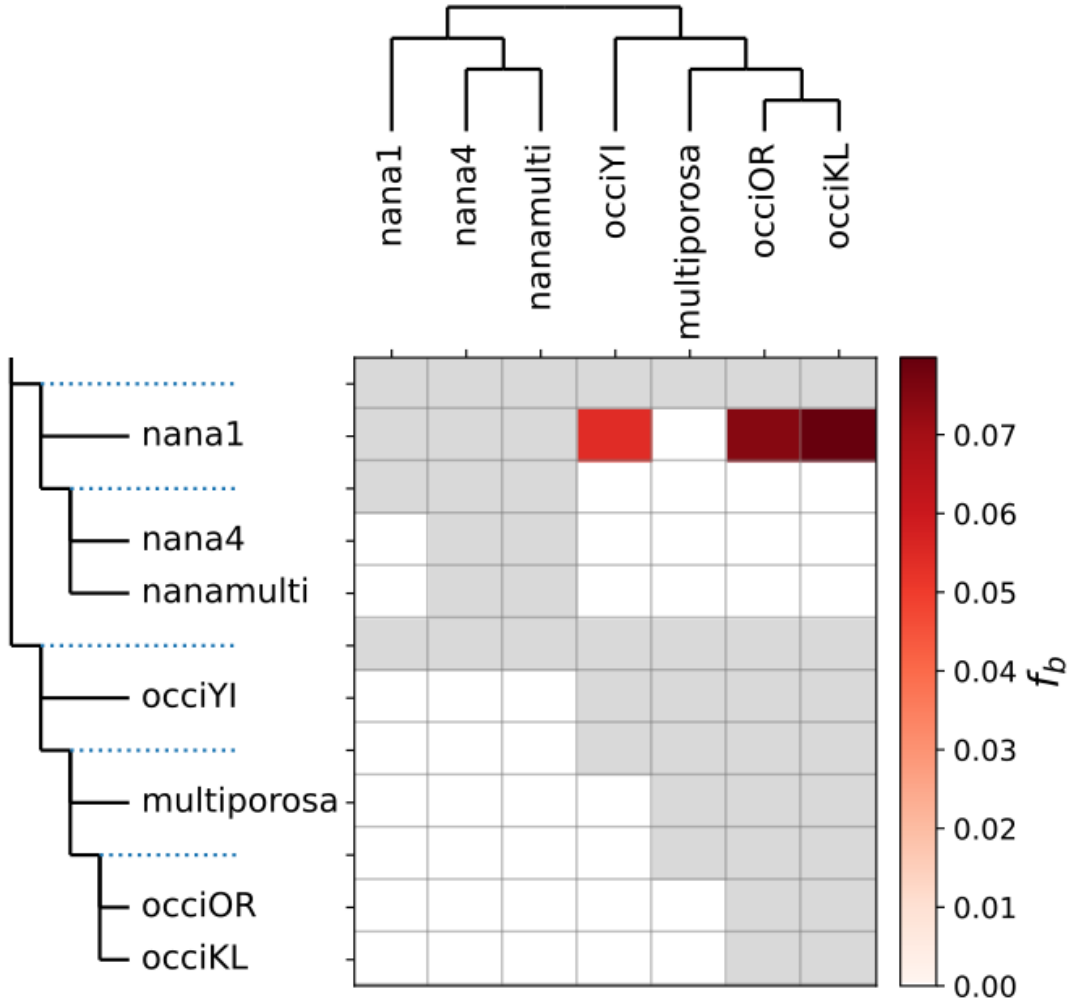

Figure 3. Excess allele sharing in the *Gehyra nana-occidentalis* clade estimated using f-branch statistics implemented in *Dsuite*. Colours indicate the proportion of introgressed loci inferred between the lineage (*x* axis) and lineage branch (*y* axis). The f-branch metric accounts for correlated allele frequencies derived from ancestral introgression using internal branches on the y-axis (dotted lines). Grey cells represent duplicate or untestable relationships. Note that despite the *ca*. 5–7% estimated excess allele sharing between *nana*1 and the three *G. occidentalis* lineages, these were not significant following P-value adjustment (Table S6).

Recent introgression at contact zones

We detected only a single early generation hybrid using NewHybrids, which was between nanamulti and *nana*4 (F1 or F2 hybrid; Table S2; Figure S1), although the sample itself did not originate from our densely sampled contact zone for that lineage pair (as shown in Figure 4b). Using sNMF, optimum K values (based on lowest ce score; Figure S6) were K = 3 for the nanamulti/nana4 contact zone, and K = 2 for the *multiporosa*/nanamulti contact zone. In the

case of the *multiporosa*/nanamulti contact zone, however, K = 2 is likely favoured over K = 3 only because of the small sample size (n = 2) for what we refer to as the Mitchell Plateau (MP) population of nanamulti (Figure 4a, S7). IBD plots show elevated pairwise F_{ST} between nanamulti samples from MP and the Theda Station (TS) population, with no indication that this is driven by introgression from *multiporosa*, which would be expected to result in relatively lower F_{ST} between some between-lineage pairs. Furthermore, the MP and TS samples form distinct clusters in the PCoA plot (Figure 4a). Considering these points, we opted to use K = 3 for this contact zone, under which sNMF inferred no admixed individuals. Similarly, there is no evidence of admixture at the *nana*4/nanamulti contact zone (Figure 4b), with IBD plots again showing no decrease in between-lineage pairwise F_{ST} as geographic distance decreases. At this contact zone there is strong geographic structure within *nana*4, with one population restricted to the King Edward (KE) sandstones and another restricted to the Morgan River (MR) sandstones.

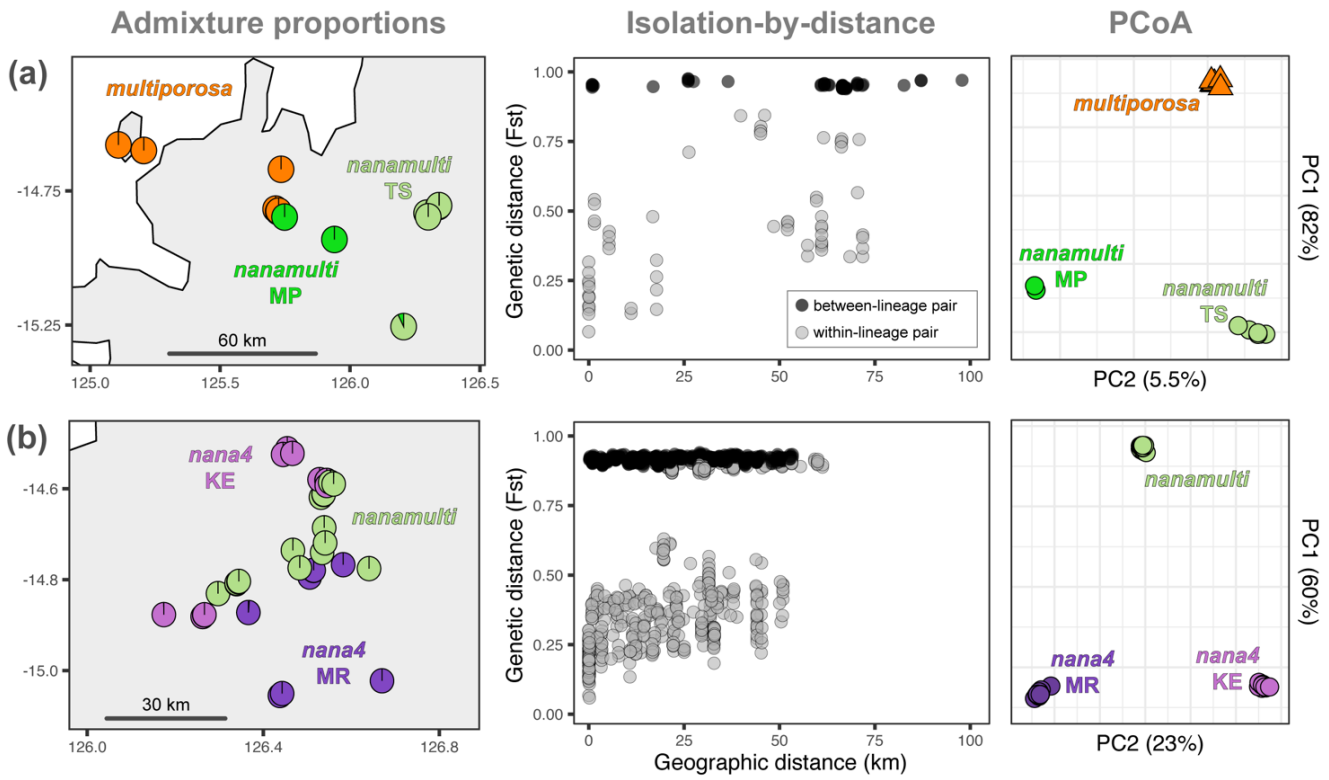

Figure 4. Estimates of gene flow at contact zones between (a) *multiporosa* and *nanamulti*, and (b) *nana*4 and *nanamulti*. Maps (left column) show pie charts that reflect individual admixture proportions estimated by sNMF (some charts are slightly offset for visibility). Isolation-by-distance plots (middle column) illustrate within-lineage (grey) and between-lineage (black). Principal coordinates analysis plots (right column) illustrate the major axes of genomic variation for the respective samples. Note that one lineage at each contact zone is represented by two within-lineage populations, reflecting strong within-lineage geographic structure.

Phenotypic variation

There was significant morphological divergence among lineages (RRPP: $df = 6/173$ $F = 107.7$, $Z = 17.19$, $R^2 = 0.789$, $P < 0.001$), with lineage accounting for 79% of observed morphological variation. Subsequent pairwise comparisons between lineages found all lineage comparisons – with the exceptions of *multiporosa* + *occidentalis*-OR, *nana*1 + nanamulti, *nana*4 + nanamulti, and all *occidentalis* lineage comparisons – to be significantly different ($P < 0.05$; Table S7). Principal components (PC) axes indicate that body size is the main axis of morphological variation among lineages (Figure 5), with all traits loading heavily on PC1 (Table S8), which accounts for 95% of morphological variation. Body shape overlapped considerably among lineages (Figure 5). PC2 explained only 1.1% of variation, with head depth loading most heavily. PC3 explained 0.96% of variation, with (in descending order) width-between-eyes, forelimb length, and hindlimb length loading most heavily. A total of 98% of morphological variation was explained by PC1–3 (Table S8). Finally, while body size varied among lineages, there were no significant differences in body size variance among lineages (Fligner-Killeen test: $X^2 = 11.749$, $df = 6$, $P = 0.068$).

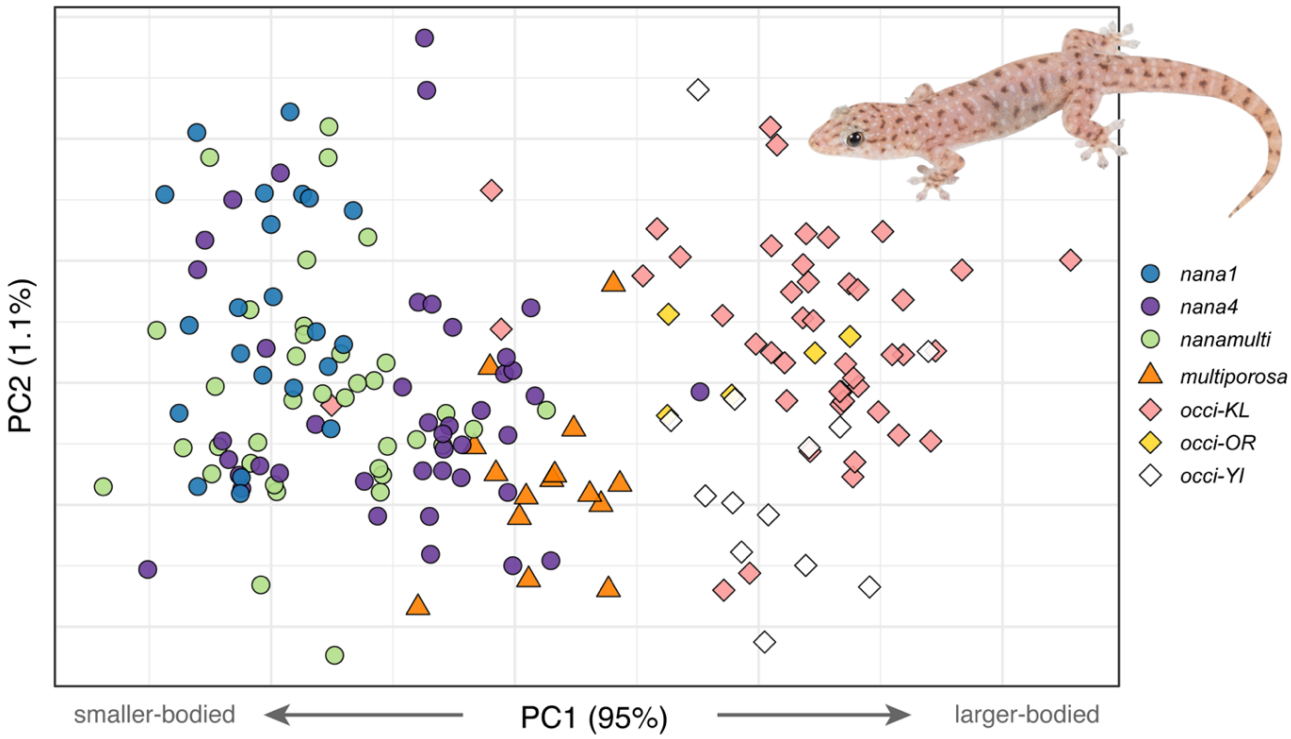

Figure 5. Principal Components Analysis of morphological variation across focal lineages in the *Gehyra nana-occidentalis* clade. Individuals are coloured according to their nuDNA ancestry. Percent variation explained for each axis. An individual of *nana1* is shown (credit: Scott Macor).

Discussion

In this study we found extensive, within-lineage mitonuclear discordance consistent with repeated mitochondrial introgression from *G. multiporosa* to nanamulti. We also confirmed phylogenetic-scale mitonuclear discordance in the *G. occidentalis* complex that could reflect either of two equivocal scenarios of mtDNA introgression, although here mtDNA introgression, rather than ILS, is less certain than between *multiporosa* and nanamulti. Despite these cases of mitonuclear discordance, phylogenetic network analysis strongly supported only a single instance of modest nuDNA introgression — from nanamulti to *multiporosa* (Figure 2), in the opposite direction to mitochondrial capture — but with no congruent support from *D*-statistics. Furthermore, we found no evidence of recent or ongoing introgression between lineages at the two contact zones examined here (Figure 5), including between *multiporosa* and nanamulti where they currently co-occur; although we did detect a single early generation hybrid between *nana*4 and nanamulti. Finally, we found no evidence of novel, intermediate, or more variable morphological traits in lineages with mitonuclear discordance. Collectively, these results highlight a system with clear evidence of repeated hybridisation and mtDNA capture but with no overt evidence of other genotypic or phenotypic consequences. We note that our use of protein-coding exon data could have missed introgressed regions of the genome; however, we might still have expected our *Dsuite* analysis, which used genome-wide SNP data, to identify potential nuDNA introgression. Further studies in this system could use complete genome sequencing to compare nuDNA regions associated with mitonuclear interactions, as co-introgression of these alleles may be necessary to maintain mitochondrial performance (Ding et al., 2021; Nikelski et al., 2023).

Mitonuclear discordance but no substantial nuclear introgression

Mitonuclear discordance is often an indicator of mtDNA introgression (Toews & Brelsford, 2012) and frequently predicts matching nuDNA introgression (e.g., Sarver et al., 2021; Ji et al., 2023; Potter et al., 2024). However, widespread mtDNA introgression can also occur with comparatively low levels of nuDNA introgression (Chan & Levin, 2005; Sloan et al., 2017). Here, our results add to a growing body of evidence demonstrating mtDNA introgression with little concomitant nuDNA introgression, which has been identified widely across taxa (e.g., Nevado et al., 2009; Boratyński et al., 2015; Good et al., 2015; Grummer et al., 2018; Mao & Rossiter, 2020). However, complete, recurrent mtDNA replacement with no detected nuDNA introgression – as

observed here for nanamulti – seems markedly rarer and, to the best of our knowledge, has only been reported in *Lissotriton* newts (Zieliński et al., 2013).

Mitochondrial genomes can easily cross species boundaries following hybridisation due to a lack of recombination and uniparental inheritance (Vargas et al., 2017; Zhang et al., 2019). Within the *nana-occidentalis* clade, mitonuclear discordance observed within nanamulti itself implies multiple, recent introgression events from *multiporosa*. Despite this, we detected only small amounts of nuDNA introgression (~5%) and in the opposite direction — from nanamulti to *multiporosa* — to what was expected given the direction of mtDNA introgression. The discordance within the *occidentalis* complex is more difficult to interpret and could be explained by mtDNA capture from *multiporosa* to *occidentalis*-OR or from *occidentalis*-YI to *occidentalis*-KL — or even by estimation error or incomplete lineage sorting. In this case, we found no evidence of nuDNA introgression to match either scenario of mtDNA introgression. Despite a general lack of nuDNA introgression shown here, repeated instances of mtDNA capture indicate that hybridisation is, or has been, relatively frequent in the *nana-occidentalis* clade. Phylogenies inferred from mtDNA are expected to achieve reciprocal monophyly more quickly than nuDNA due to the smaller effective population size and elevated mutation rates of mtDNA (Ballard & Whitlock, 2004). This suggests that the mtDNA introgression events from *multiporosa* to nanamulti have been recent given the rampant mtDNA paraphyly within these lineages. Thus, nuDNA introgression was either swiftly purged or extremely limited following these introgression events.

Several factors may explain the lack of nuDNA introgression observed here. Adaptive introgression of mtDNA is frequently cited to drive asymmetrical patterns of mtDNA vs nuDNA introgression (Toews & Brelsford, 2012; Bonnet et al., 2017; Sloan et al., 2017) and has been identified in *Lepus* hares (Melo-Ferreira et al., 2014), *Drosophila* flies (Llopart et al., 2014), and *Myodes* voles (Boratyński et al., 2015), among other taxa. However, confident identification of adaptive introgression requires the demonstration of adaptive function, which is often difficult (Toews et al., 2013; Taylor & Larson, 2019). Detection methods for positive selection (e.g., Suarez-Gonzalez et al., 2018) must be used with caution, as phenomena such as heterosis can mimic signals of adaptive introgression (Kim et al., 2017). Alternatively, demographic processes such as gene surfing — whereby markers more prone to drift, such as mtDNA, are fixed in populations undergoing rapid range expansion (Excoffier et al., 2009) — may have driven the fixation of *multiporosa* mtDNA in nanamulti, as there is evidence of range expansion in nanamulti (Lau et al., 2025). Similar introgression scenarios driven by range expansion have been detected in groups such as *Otospermophilus* ground squirrels (Phuong et al., 2017) and *Ursus* bears

(Cahill et al., 2013). However, range expansion would not account for the fixation of *multiporosa* mtDNA over the entirety of the range of the nanamulti lineage, and demographic processes generally have been suggested to cause massive discordance only rarely (see Bonnet et al., 2017).

Introgression and morphology

Despite a growing number of studies demonstrating the potential role introgression can play in generating morphological variation (e.g., Lamichhaney et al., 2015; Taylor & Larson, 2019), we found no association between introgression and phenotypic variation in the *nana-occidentalis* clade in terms of the morphometric characters we measured. However, given the lack of nuDNA introgression found here, it is not surprising that we found no evidence for transgressive, intermediate, or more variable phenotypes. In other cases where introgression has been suggested to influence morphology in squamates (e.g., Pavón-Vázquez et al., 2021; Wogan et al., 2023) the estimated proportion of introgression was significantly higher than what was found here. In line with other studies of *Gehyra* morphology (see Sistrom et al., 2012; Kealley et al., 2018; Moritz et al., 2018), our results highlighted body size as the main axis of among-lineage morphological variation in the *nana-occidentalis* clade. Considering this, it is worth noting that *multiporosa* is somewhat intermediate in body size with respect to the *nana* and *occidentalis* complexes. This could have facilitated hybridisation with nanamulti or it could, conceivably, be the result of introgression; however, this is unlikely considering the modest nuDNA introgression estimated using the MSCi, and the lack of introgression detected with *D*-statistics.

Conclusions and future directions

Methods to infer genomic introgression have improved and diversified over the last two decades and, given the biases and limitations unique to each method, comparing the results of multiple analyses is often warranted to ensure that results are robust (Hibbins & Hahn, 2022). Here, we used several such methods to understand the complicated evolutionary history of a clade of *Gehyra* geckos. These results highlight a system with repeated instances of asymmetrical mtDNA introgression with limited evidence of corresponding nuDNA introgression. Mitonuclear discordance and introgression have now been widely identified in squamates (e.g., Grummer et al., 2018; Prates et al., 2023; Wogan et al., 2023; Myers et al., 2024), however, in none of these instances has the disparity between levels of mtDNA and nuDNA introgression been so clearly demonstrated. More work in this and other systems is needed to understand whether such mismatches result from selection or non-adaptive factors. Such studies could also assess the

potential for mtDNA introgression to drive speciation by providing adaptive benefit, or by introducing mitonuclear interactions that reinforce RI between diverging lineages. Whole genome sequencing is more accessible than ever and will be needed to answer such questions (Combrink et al., 2025).

Acknowledgments

We thank Scott Macor and Naomi Laven for assistance with field sampling; Adam Leaché, Emily Roycroft, Kate O'Hara, and Rhiannon Schembri for advice; Rhiannon Schembri for assistance with lab work; Paul Doughty and Kailah Thorn of the Western Australian Museum for access to tissues and specimens; and Scott Macor and Ian Bool for providing photos. This work was funded by Australian Research Council Discovery Projects DP190102395 and DP210102267, and an Australian Biological Resources Study NTRGP Postdoctoral Fellowship Grant to SMZ (NTRGI000036).

References

Abbott, R., Albach, D., Ansell, S., Arntzen, J. W., Baird, S. J., Bierne, N., Boughman, J., Brelsford, A., Buerkle, C. A., Buggs, R., Butlin, R. K., Dieckmann, U., Eroukhmanoff, F., Grill, A., Cahan, S. H., Hermansen, J. S., Hewitt, G., Hudson, A. G., Jiggins, C., Jones, J., Keller, B., Marczewski, T., Mallet, J., Martinez-Rodriguez, P., Möst, M., Mullen, S., Nichols, R., Nolte, A. W., Parisod, C., Pfennig, K., Rice, A. M., Ritchie, M. G., Seifert, B., Smadja, C. M., Stelkens, R., Szymura, J. M., Väinölä, R., Wolf, J. B., & Zinner, D. (2013). Hybridization and speciation. *Journal of Evolutionary Biology*, 26(2), 229–246. https://doi.org/10.1111/j.1420-9101.2012.02599.x

Anderson, E., & Thompson, E. (2002). A model-based method for identifying species hybrids using multilocus genetic data. *Genetics*, 160(3), 1217–1229.

Ashman, L., Bragg, J., Doughty, P., Hutchinson, M., Bank, S., Matzke, N., Oliver, P., & Moritz, C. (2018). Diversification across biomes in a continental lizard radiation. *Evolution*, 72(8), 1553–1569.

Ballard, J. W., & Whitlock, M. C. (2004). The incomplete natural history of mitochondria. *Molecular Ecology*, 13(4), 729–744. https://doi.org/10.1046/j.1365-294x.2003.02063.x

Barley, A. J., Nieto-Montes de Oca, A., Manríquez-Morán, N. L., & Thomson, R. C. (2024). Understanding Species Boundaries that Arise from Complex Histories: Gene Flow Across the Speciation Continuum in the Spotted Whiptail Lizards. *Systematic Biology*, 73(6), 901–919.

Benjamini, Y., & Hochberg, Y. (1995). Controlling the False Discovery Rate: A Practical and Powerful Approach to Multiple Testing. *Journal of the Royal Statistical Society: Series B (Methodological)*, 57(1), 289–300. https://doi.org/10.1111/j.2517-6161.1995.tb02031.x

Blom, M. P. (2015). EAPhy: a flexible tool for high-throughput quality filtering of exon-alignments and data processing for phylogenetic methods. *PLoS Currents*, 5(7). https://doi.org/10.1371/currents.tol.75134257bd389c04bc1d26d42aa9089f

Bonnet, T., Leblois, R., Rousset, F., & Crochet, P. A. (2017). A reassessment of explanations for discordant introgressions of mitochondrial and nuclear genomes. *Evolution*, 71(9), 2140–2158.

Boratyński, Z., Melo-Ferreira, J., Alves, P., Berto, S., Koskela, E., Pentikäinen, O., Tarroso, P., Ylilauri, M., & Mappes, T. (2014). Molecular and ecological signs of mitochondrial adaptation: consequences for introgression? *Heredity*, 113(4), 277–286.

Bradburd, G. (2013). Package 'BEDASSLE'. Comprehensive R Archive Network.

Cahill, J. A., Green, R. E., Fulton, T. L., Stiller, M., Jay, F., Ovsyanikov, N., Salamzade, R., St. John, J., Stirling, I., & Slatkin, M. (2013). Genomic evidence for island population conversion resolves conflicting theories of polar bear evolution. *PLoS Genetics*, 9(3), e1003345.

Chan, K. M. A., & Levin, S. A. (2005). Leaky prezygotic isolation and porous genomes: rapid introgression of maternally inherited DNA. *Evolution*, 59(4), 720–729. https://doi.org/10.1111/j.0014-3820.2005.tb01748.x

Collyer, M. L., Sekora, D. J., & Adams, D. C. (2015). A method for analysis of phenotypic change for phenotypes described by high-dimensional data. *Heredity*, 115(4), 357–365. https://doi.org/10.1038/hdy.2014.75

Combrink, L. L., Golcher-Benavides, J., Lewanski, A. L., Rick, J. A., Rosenthal, W. C., & Wagner, C. E. (2025). Population Genomics of Adaptive Radiation. *Molecular Ecology*, 34, e17574.

Cooper, E. D. (2014). Overly simplistic substitution models obscure green plant phylogeny. *Trends in Plant Science*, 19(9), 576–582.

Cruickshank, T. E., & Hahn, M. W. (2014). Reanalysis suggests that genomic islands of speciation are due to reduced diversity, not reduced gene flow. *Molecular Ecology*, 23(13), 3133–3157.

Currat, M., Ruedi, M., Petit, R. J., & Excoffier, L. (2008). The hidden side of invasions: massive introgression by local genes. *Evolution*, 62(8), 1908–1920. https://doi.org/10.1111/j.1558-5646.2008.00413.x

Dickey, M. (1971). The weighted likelihood ratio, linear hypotheses on normal location parameters. *The Annals of Mathematical Statistics*, 42(1), 204–223.

Ding, Y., Chen, W., Li, Q., Rossiter, S. J., & Mao, X. (2021). Mitonuclear mismatch alters nuclear gene expression in naturally introgressed *Rhinolophus bats*. *Frontiers in Zoology*, 18, 1–14.

Dittrich-Reed, D. R., & Fitzpatrick, B. M. (2013). Transgressive hybrids as hopeful monsters. *Evolutionary Biology*, 40, 310–315.

Dixon, P. (2003). VEGAN, a package of R functions for community ecology. *Journal of Vegetation Science,* 14, 927–930. https://doi.org/10.1658/1100-9233(2003)014[0927:VAPORF]2.0.CO;2

Doughty, P., Bourke, G., Tedeschi, L. G., Pratt, R. C., Oliver, P. M., Palmer, R. A., & Moritz, C. (2018). Species delimitation in the *Gehyra nana* (Squamata: Gekkonidae) complex: cryptic and divergent

morphological evolution in the Australian Monsoonal Tropics, with the description of four new species. *Zootaxa*, 4403(2), 201–244. https://doi.org/10.11646/zootaxa.4403.2.1

Doughty, P., Palmer, R., Sistrom, M. J., Bauer, A. M., & Donnellan, S. C. (2012). Two new species of *Gehyra* (Squamata: Gekkonidae) geckos from the north-west Kimberley region of Western Australia. *Records of the Western Australian Museum*, 27(2), 117–134.

Durand, E. Y., Patterson, N., Reich, D., & Slatkin, M. (2011). Testing for ancient admixture between closely related populations. *Molecular Biology and Evolution*, 28(8), 2239–2252. https://doi.org/10.1093/molbev/msr048

Edelman, N. B., & Mallet, J. (2021). Prevalence and Adaptive Impact of Introgression. *Annual Review of Genetics*, 55, 265–283. https://doi.org/10.1146/annurev-genet-021821-020805

Excoffier, L., Foll, M., & Petit, R. J. (2009). Genetic consequences of range expansions. *Annual Review of Ecology, Evolution, and Systematics*, 40(1), 481–501.

Fenker, J., Tedeschi, L. G., Melville, J., & Moritz, C. (2021). Predictors of phylogeographic structure among codistributed taxa across the complex Australian monsoonal tropics. *Molecular Ecology*, 30(17), 4276–4291. https://doi.org/10.1111/mec.16057

Fligner, M. A., & Killeen, T. J. (1976). Distribution-Free Two-Sample Tests for Scale. *Journal of the American Statistical Association,* 71(353), 210–213. https://doi.org/10.2307/2285771

Flouri, T., Jiao, X., Rannala, B., & Yang, Z. (2018). Species Tree Inference with BPP Using Genomic Sequences and the Multispecies Coalescent. *Molecular Biology and Evolution*, 35(10), 2585–2593. https://doi.org/10.1093/molbev/msy147

Flouri, T., Jiao, X., Rannala, B., & Yang, Z. (2020). A Bayesian Implementation of the Multispecies Coalescent Model with Introgression for Phylogenomic Analysis. *Molecular Biology and Evolution*, 37(4), 1211–1223. https://doi.org/10.1093/molbev/msz296

Frichot, E., Mathieu, F., Trouillon, T., Bouchard, G., François, O. (2014). Fast and Efficient Estimation of Individual Ancestry Coefficients. *Genetics*, 196(4), 973–983. https://doi.org/10.1534/genetics.113.160572

Frichot, E., & François, O. (2015). LEA: An R Package for Landscape and Ecological Association Studies. *Methods in Ecology and Evolution*, 6(8), 925–929. https://doi.org/10.1111/2041-210X.12382

Gadagkar, S. R., Rosenberg, M. S., & Kumar, S. (2005). Inferring species phylogenies from multiple genes: concatenated sequence tree versus consensus gene tree. *Journal of Experimental Zoology Part B: Molecular and Developmental Evolution*, 304(1), 64–74.

Galtier, N., & Daubin, V. (2008). Dealing with incongruence in phylogenomic analyses. *Philosophical Transactions of the Royal Society B: Biological Sciences*, 363(1512), 4023–4029.

Good, J. M., Vanderpool, D., Keeble, S., & Bi, K. (2015). Negligible nuclear introgression despite complete mitochondrial capture between two species of chipmunks. *Evolution*, 69(8), 1961–1972.

690 Gruber, B., Unmack, P. J., Berry, O. F., & Georges, A. (2018). dartr: An r package to facilitate analysis of SNP
691 data generated from reduced representation genome sequencing. *Molecular Ecology Resources,* 18(3),
692 691–699.
693 Grummer, J. A., Morando, M. M., Avila, L. J., Sites, J. W., & Leaché, A. D. (2018). Phylogenomic evidence for
694 a recent and rapid radiation of lizards in the Patagonian *Liolaemus fitzingerii* species group. *Molecular*
695 *Phylogenetics and Evolution*, 125, 243–254.
696 https://doi.org/https://doi.org/10.1016/j.ympev.2018.03.023
697 Guindon, S., Dufayard, J.-F., Lefort, V., Anisimova, M., Hordijk, W., & Gascuel, O. (2010). New algorithms
698 and methods to estimate maximum-likelihood phylogenies: assessing the performance of PhyML 3.0.
699 *Systematic Biology*, 59(3), 307–321.
700 Harrison, R. G., & Larson, E. L. (2014). Hybridization, introgression, and the nature of species boundaries.
701 *Journal of Heredity*, 105(S1), 795–809.
702 Heinicke, M., Greenbaum, E., Jackman, T., & Bauer, A. (2011). Phylogeny of a trans-Wallacean radiation
703 (Squamata, Gekkonidae, *Gehyra*) supports a single early colonization of Australia. *Zoologica Scripta*,
704 40, 584–602. https://doi.org/10.1111/j.1463-6409.2011.00495.x
705 Hibbins, M. S., & Hahn, M. W. (2022). Phylogenomic approaches to detecting and characterizing
706 introgression. *Genetics*, 220(2), iyab173. https://doi.org/10.1093/genetics/iyab173
707 Hill, G. E. (2019). Reconciling the mitonuclear compatibility species concept with rampant mitochondrial
708 introgression. *Integrative and Comparative Biology*, 59(4), 912–924.
709 Hillis, D. M., Chambers, E. A., & Devitt, T. J. (2021). Contemporary methods and evidence for species
710 delimitation. *Ichthyology & Herpetology*, 109(3), 895–903.
711 Hoang, D. T., Chernomor, O., Von Haeseler, A., Minh, B. Q., & Vinh, L. S. (2018). UFBoot2: improving the
712 ultrafast bootstrap approximation. *Molecular Biology and Evolution*, 35(2), 518–522.
713 Hodcroft, E. (2016). TreeCollapserCL4. Retrieved 10/05/2023 from
714 http://emmahodcroft.com/TreeCollapseCL.html
715 Huang, J., Thawornwattana, Y., Flouri, T., Mallet, J., & Yang, Z. (2022). Inference of Gene Flow between
716 Species under Misspecified Models. *Molecular Biology and Evolution*, 39(12), msac237.
717 https://doi.org/10.1093/molbev/msac237
718 Ji, J., Jackson, D. J., Leaché, A. D., & Yang, Z. (2023). Power of Bayesian and Heuristic Tests to Detect
719 Cross-Species Introgression with Reference to Gene Flow in the *Tamias quadrivittatus* Group of North
720 American Chipmunks. *Systematic Biology*, 72(2), 446–465. https://doi.org/10.1093/sysbio/syac077
721 Kalyaanamoorthy, S., Minh, B. Q., Wong, T. K. F., von Haeseler, A., & Jermiin, L. S. (2017). ModelFinder: fast
722 model selection for accurate phylogenetic estimates. *Nature Methods*, 14(6), 587–589.
723 https://doi.org/10.1038/nmeth.4285
724 Kealley, L., Doughty, P., Pepper, M., Keogh, J. S., Hillyer, M., & Huey, J. (2018). Conspicuously concealed:
725 revision of the arid clade of the *Gehyra variegata* (Gekkonidae) group in Western Australia using an

integrative molecular and morphological approach, with the description of five cryptic species. *PeerJ*, 6, e5334. https://doi.org/10.7717/peerj.5334

Kilian, A., Wenzl, P., Huttner, E., Carling, J., Xia, L., Blois, H., Caig, V., Heller-Uszynska, K., Jaccoud, D., Hopper, C., Aschenbrenner-Kilian, M., Evers, M., Peng, K., Cayla, C., Hok, P., Uszynski, G. (2012). Diversity arrays technology: a generic genome profiling technology on open platforms. *Data production and analysis in population genomics: Methods and protocols,* 67–89.

Kim, B. Y., Huber, C. D., & Lohmueller, K. E. (2017). Deleterious variation mimics signatures of genomic incompatibility and adaptive introgression. *PLOS Genetics*, 14(10), e1007741. https://doi.org/10.1371/journal.pgen.1007741

Lamichhaney, S., Berglund, J., Almén, M. S., Maqbool, K., Grabherr, M., Martinez-Barrio, A., Promerová, M., Rubin, C. J., Wang, C., Zamani, N., Grant, B. R., Grant, P. R., Webster, M. T., & Andersson, L. (2015). Evolution of Darwin's finches and their beaks revealed by genome sequencing. *Nature*, 518(7539), 371–375. https://doi.org/10.1038/nature14181

Lanfear, R., Calcott, B., Ho, S. Y., & Guindon, S. (2012). PartitionFinder: combined selection of partitioning schemes and substitution models for phylogenetic analyses. *Molecular Biology and Evolution,* 29(6), 1695–1701.

Larson, D. A., Itgen, M., Denton, R., & Hahn, M. W. (preprint). Reconsidering cytonuclear discordance in the genomic age. *EcoEvoRxiv.* https://doi.org/https://doi.org/10.32942/X2KG8R

Lau, C. C., Christian, K. A., Fenker, J., Laver, R. J., O'Hara, K., Zozaya, S. M., Moritz, C., & Roycroft, E. (2025). Range size variably predicts genetic diversity in *Gehyra* geckos. *Evolution*, qpaf057. https://doi.org/10.1093/evolut/qpaf057

Lawson, D. J., van Dorp, L., & Falush, D. (2018). A tutorial on how not to over-interpret STRUCTURE and ADMIXTURE bar plots. *Nature Communications*, 9(1), 3258. https://doi.org/10.1038/s41467-018-05257-7

Llopart, A., Herrig, D., Brud, E., & Stecklein, Z. (2014). Sequential adaptive introgression of the mitochondrial genome in *Drosophila yakuba* and *Drosophila santomea*. *Molecular Ecology*, 23(5), 1124–1136.

Malinsky, M., Matschiner, M., & Svardal, H. (2021). Dsuite - Fast D-statistics and related admixture evidence from VCF files. *Molecular Ecology Resources,* 21(2), 584–595. https://doi.org/10.1111/1755-0998.13265

Mallet, J., Besansky, N., & Hahn, M. W. (2016). How reticulated are species? *BioEssays*, 38(2), 140–149.

Mao, X., & Rossiter, S. J. (2020). Genome-wide data reveal discordant mitonuclear introgression in the intermediate horseshoe bat (*Rhinolophus affinis*). *Molecular Phylogenetics and Evolution*, 150, 106886.

Masello, J. F., Quillfeldt, P., Sandoval-Castellanos, E., Alderman, R., Calderón, L., Cherel, Y., Cole, T. L., Cuthbert, R. J., Marin, M., & Massaro, M. (2019). Additive traits lead to feeding advantage and

reproductive isolation, promoting homoploid hybrid speciation. *Molecular Biology and Evolution*, 36(8), 1671–1685.

Mayr, E. (1963). Animal species and evolution. *Harvard University Press*.

Melo-Ferreira, J., Vilela, J., Fonseca, M. M., da Fonseca, R. R., Boursot, P., & Alves, P. C. (2014). The elusive nature of adaptive mitochondrial DNA evolution of an arctic lineage prone to frequent introgression. *Genome Biology and Evolution*, 6(4), 886–896.

Minh, B. Q., Schmidt, H. A., Chernomor, O., Schrempf, D., Woodhams, M. D., Von Haeseler, A., & Lanfear, R. (2020). IQ-TREE 2: new models and efficient methods for phylogenetic inference in the genomic era. *Molecular Biology and Evolution*, 37(5), 1530–1534.

Moritz, C. C., Pratt, R. C., Bank, S., Bourke, G., Bragg, J. G., Doughty, P., Keogh, J. S., Laver, R. J., Potter, S., Teasdale, L. C., Tedeschi, L. G., & Oliver, P. M. (2018). Cryptic lineage diversity, body size divergence, and sympatry in a species complex of Australian lizards (*Gehyra*). *Evolution*, 72(1), 54–66. https://doi.org/10.1111/evo.13380

Myers, E., Rautsaw, R., Borja, M., Jones, J., Grunwald, C., Holding, M., Grazziotin, F., & Parkinson, C. (2024). Phylogenomic discordance is driven by widespread introgression and incomplete lineage sorting during rapid species diversification within Rattlesnakes (Viperidae: *Crotalus* and *Sistrurus*). *Systematic Biology*, 73(4), 722–741.

Nevado, B., Koblmüller, S., Sturmbauer, C., Snoeks, J., Usano-Alemany, J., & Verheyen, E. (2009). Complete mitochondrial DNA replacement in a Lake Tanganyika cichlid fish. *Molecular Ecology,* 18(20), 4240–4255.

Nikelski, E., Rubtsov, A. S., & Irwin, D. (2023). High heterogeneity in genomic differentiation between phenotypically divergent songbirds: a test of mitonuclear co-introgression. *Heredity*, 130(1), 1–13.

Oliver, P., Laver, R., Martins, F., Pratt, R., Hunjan, S., & Moritz, C. (2016). A novel hotspot of vertebrate endemism and an evolutionary refugium in tropical Australia. *Diversity and Distributions*, 23(1), 53–66. https://doi.org/10.1111/ddi.12506

Oliver, P. M., Prasetya, A. M., Tedeschu, L. G., Fenker, J., Ellis, R. J., Doughty, P., & Moritz, C. (2020). Crypsis and convergence: integrative taxonomic revision of the *Gehyra australis* group (Squamata: Gekkonidae) from northern Australia. *PeerJ*, 8, e7971. https://doi.org/10.7717/peerj.7971

Oliver, P. M., Ashman, L. G., Bank, S., Laver, R. J., Pratt, R. C., Tedeschi, L. G., & Moritz, C. (2019). On and off the rocks: persistence and ecological diversification in a tropical Australian lizard radiation. *BMC Evolutionary Biology*, 19, 81. https://doi.org/10.1186/s12862-019-1408-1

Patterson, N., Moorjani, P., Luo, Y., Mallick, S., Rohland, N., Zhan, Y., Genschoreck, T., Webster, T., & Reich, D. (2012). Ancient admixture in human history. *Genetics*, 192(3), 1065–1093.

Pavón-Vázquez, C. J., Rana, Q., Farleigh, K., Crispo, E., Zeng, M., Liliah, J., Mulcahy, D., Ascanio, A., Jezkova, T., & Leaché, A. D. (2024). Gene Flow and Isolation in the Arid Nearctic Revealed by Genomic Analyses of Desert Spiny Lizards. *Systematic Biology*, 73(2), 323–342. https://doi.org/10.1093/sysbio/syae001

Pfennig, K. S., Kelly, A. L., & Pierce, A. A. (2016). Hybridization as a facilitator of species range expansion. *Proceedings of the Royal Society B: Biological Sciences*, 283(1839). https://doi.org/10.1098/rspb.2016.1329

Phuong, M. A., Bi, K., & Moritz, C. (2017). Range instability leads to cytonuclear discordance in a morphologically cryptic ground squirrel species complex. *Molecular Ecology*, 26(18), 4743–4755.

Potter, S., Moritz, C., Piggott, M. P., Bragg, J. G., Afonso Silva, A. C., Bi, K., McDonald-Spicer, C., Turakulov, R., & Eldridge, M. D. (2024). Museum skins enable identification of introgression associated with cytonuclear discordance. *Systematic Biology*, 73(3), 579–593. https://doi.org/10.1093/sysbio/syae016

Prates, I., Hutchinson, M. N., Singhal, S., Moritz, C., & Rabosky, D. L. (2023). Notes from the taxonomic disaster zone: Evolutionary drivers of intractable species boundaries in an Australian lizard clade (Scincidae: *Ctenotus*). *Molecular Ecology,* 33(20), e17074. https://doi.org/10.1111/mec.17074

Puechmaille, S. J. (2016). The program structure does not reliably recover the correct population structure when sampling is uneven: subsampling and new estimators alleviate the problem. *Molecular Ecology Resources,* 16(3), 608–627. https://doi.org/10.1111/1755-0998.12512

Rabiee, M., Sayyari, E., & Mirarab, S. (2019). Multi-allele species reconstruction using ASTRAL. *Molecular Phylogenetics and Evolution*, 130, 286–296. https://doi.org/https://doi.org/10.1016/j.ympev.2018.10.033

Rambaut, A., Drummond, A. J., Xie, D., Baele, G., & Suchard, M. A. (2018). Posterior summarization in Bayesian phylogenetics using Tracer 1.7. *Systematic Biology*, 67(5), 901–904.

Rhymer, J. M., & Simberloff, D. (1996). Extinction by Hybridization and Introgression. *Annual Review of Ecology and Systematics*, 27, 83–109. http://www.jstor.org/stable/2097230

Sansaloni, C. P., Petroli, C. D., Carling, J., Hudson, C. J., Steane, D. A., Myburg, A. A., Grattapaglia, D., Vaillancourt, R. E., & Kilian, A. (2010). A high-density Diversity Arrays Technology (DArT) microarray for genome-wide genotyping in Eucalyptus. *Plant Methods*, 6, 1–11.

Sarver, B. A. J., Herrera, N. D., Sneddon, D., Hunter, S. S., Settles, M. L., Kronenberg, Z., Demboski, J. R., Good, J. M., & Sullivan, J. (2021). Diversification, Introgression, and Rampant Cytonuclear Discordance in Rocky Mountains Chipmunks (Sciuridae: *Tamias*). *Systematic Biology*, 70(5), 908–921. https://doi.org/10.1093/sysbio/syaa085

Schumer, M., Rosenthal, G. G., & Andolfatto, P. (2014). How common is homoploid hybrid speciation? *Evolution*, 68(6), 1553–1560. https://doi.org/10.1111/evo.12399

Seo, T.-K., Kishino, H., & Thorne, J. L. (2005). Incorporating gene-specific variation when inferring and evaluating optimal evolutionary tree topologies from multilocus sequence data. *Proceedings of the National Academy of Sciences*, 102(12), 4436–4441.

Simmons, M. P., & Gatesy, J. (2021). Collapsing dubiously resolved gene-tree branches in phylogenomic coalescent analyses. *Molecular Phylogenetics and Evolution*, 158, 107092. https://doi.org/https://doi.org/10.1016/j.ympev.2021.107092

Sistrom, M., Edwards, D. L., Donnellan, S., & Hutchinson, M. (2012). Morphological differentiation correlates with ecological but not with genetic divergence in a *Gehyra* gecko. *Journal of Evolutionary Biology*, 25(4), 647–660. https://doi.org/10.1111/j.1420-9101.2012.02460.x

Sistrom, M., Hutchinson, M., Hutchinson, R., & Donnellan, S. (2009). Molecular Phylogeny Of Australian *Gehyra* (Squamata: Gekkonidae) And Taxonomic Revision Of *Gehyra variegata* In South-Eastern Australia. *Zootaxa*, 2277, 14–32. https://doi.org/10.5281/zenodo.191131

Sloan, D. B., Havird, J. C., & Sharbrough, J. (2017). The on-again, off-again relationship between mitochondrial genomes and species boundaries. *Molecular Ecology*, 26(8), 2212–2236.

Smith, M. L., & Hahn, M. W. (2024). Selection leads to false inferences of introgression using popular methods. *Genetics*, 227(4), iyae089.

Srivathsan, A., Lee, L., Katoh, K., Hartop, E., Kutty, S. N., Wong, J., Yeo, D., & Meier, R. (2021). ONTbarcoder and MinION barcodes aid biodiversity discovery and identification by everyone, for everyone. *BMC biology*, 19, 1–21.

Staubach, F., Lorenc, A., Messer, P. W., Tang, K., Petrov, D. A., & Tautz, D. (2012). Genome patterns of selection and introgression of haplotypes in natural populations of the house mouse (*Mus musculus*). *PLoS Genetics*, 8(8), e1002891. https://doi.org/10.1371/journal.pgen.1002891

Suarez-Gonzalez, A., Lexer, C., & Cronk, Q. C. (2018). Adaptive introgression: a plant perspective. *Biology letters*, 14(3), 20170688.

Taylor, S., & Larson, E. (2019). Insights from genomes into the evolutionary importance and prevalence of hybridization in nature. *Nature Ecology & Evolution*, 3, 170–177. https://doi.org/10.1038/s41559-018-0777-y

Todesco, M., Pascual, M. A., Owens, G. L., Ostevik, K. L., Moyers, B. T., Hübner, S., Heredia, S. M., Hahn, M. A., Caseys, C., Bock, D. G., & Rieseberg, L. H. (2016). Hybridization and extinction. *Evolutionary Applications*, 9(7), 892–908. https://doi.org/10.1111/eva.12367

Toews, D. P., & Brelsford, A. (2012). The biogeography of mitochondrial and nuclear discordance in animals. *Molecular Ecology*, 21(16), 3907–3930.

Toews, D. P., Mandic, M., Richards, J. G., & Irwin, D. E. (2013). Migration, mitochondria, and the yellow-rumped warbler. *Evolution*, 68(1), 241–255. https://doi.org/10.1111/evo.12260

Uetz, P., Freed, P., Aguilar, R., Reyes, F., Kudera, J., & Hošek, J. (2024). The Reptile Database. Retrieved 2024 from http://www.reptile-database.org

Vargas, O. M., Ortiz, E. M., & Simpson, B. B. (2017). Conflicting phylogenomic signals reveal a pattern of reticulate evolution in a recent high-Andean diversification (Asteraceae: Astereae: *Diplostephium*). *New Phytol*, 214(4), 1736–1750. https://doi.org/10.1111/nph.14530

Vavrek, M. J. (2011). Fossil: palaeoecological and palaeogeographical analysis tools. *Palaeontologia electronica*, 14(1), 16.

Wang, J. (2022). Fast and accurate population admixture inference from genotype data from a few microsatellites to millions of SNPs. *Heredity*, 129(2), 79–92.

Weir, B. S., & Cockerham, C. C. (1984). Estimating F-statistics for the analysis of population structure. *Evolution*, 1358–1370.

Weir, B. S., & Hill, W. G. (2002). Estimating F-statistics. *Annual review of genetics*, 36(1), 721–750.

Wilson, S., & Swan, G. (2020). A complete Guide to Reptiles of Australia. New Holland Publishers.

Wogan, G. O. U., Yuan, M. L., Mahler, D. L., & Wang, I. J. (2023). Hybridization and Transgressive Evolution Generate Diversity in an Adaptive Radiation of *Anolis* Lizards. *Systematic Biology*, 72(4), 874–884. https://doi.org/10.1093/sysbio/syad026

Wright, S. (1943). Isolation by distance. *Genetics*, 28(2), 114.

Zhang, D., Tang, L., Cheng, Y., Hao, Y., Xiong, Y., Song, G., Qu, Y., Rheindt, F. E., Alström, P., Jia, C., & Lei, F. (2019). "Ghost Introgression" As a Cause of Deep Mitochondrial Divergence in a Bird Species Complex. *Molecular Biology and Evolution*, 36(11), 2375–2386. https://doi.org/10.1093/molbev/msz170

Zieliński, P., Nadachowska-Brzyska, K., Wielstra, B., Szkotak, R., Covaciu-Marcov, S., Cogălniceanu, D., & Babik, W. (2013). No evidence for nuclear introgression despite complete mt DNA replacement in the Carpathian newt (*Lissotriton montandoni*). *Molecular Ecology*, 22(7), 1884–1903.

Zozaya, S. M., Macor, S. A., Schembri, R., Higgie, M., Hoskin, C. J., O'Hara, K., Lau, C. C., Read, W. J., & Moritz, C. (2024). Contact zones reveal restricted introgression despite frequent hybridization across a recent lizard radiation. *Evolution*, qpae174. https://doi.org/10.1093/evolut/qpae174

Supplementary material for: Repeated mitochondrial capture with limited genomic introgression in a lizard group

Wesley J. Read[1*], Craig Moritz[1], Rebecca J. Laver[1,2], Ching Ching Lau[1], & Stephen M. Zozaya[1]

[1]Division of Ecology and Evolution, Research School of Biology, The Australian National University, Acton, Australian Capital Territory, Australia. [2]The University of the Sunshine Coast, Moreton Bay Campus, Petrie, QLD, Australia. [*]Corresponding author: wesley.read@anu.edu.au

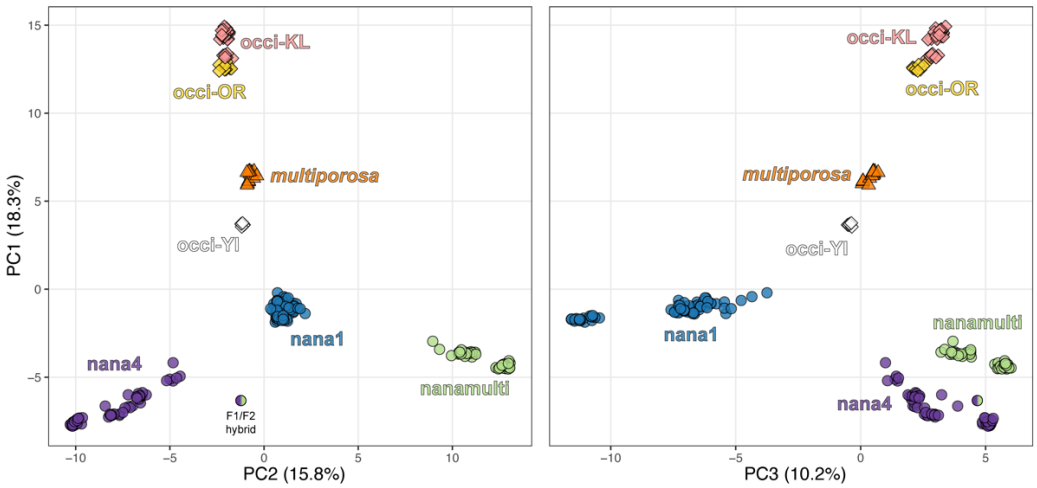

Figure S1. Ordination plots showing PC 1–3 from principal coordinates analyses (PCoA) of genome-wide SNP data across the *Gehyra nana-occidentalis* group.

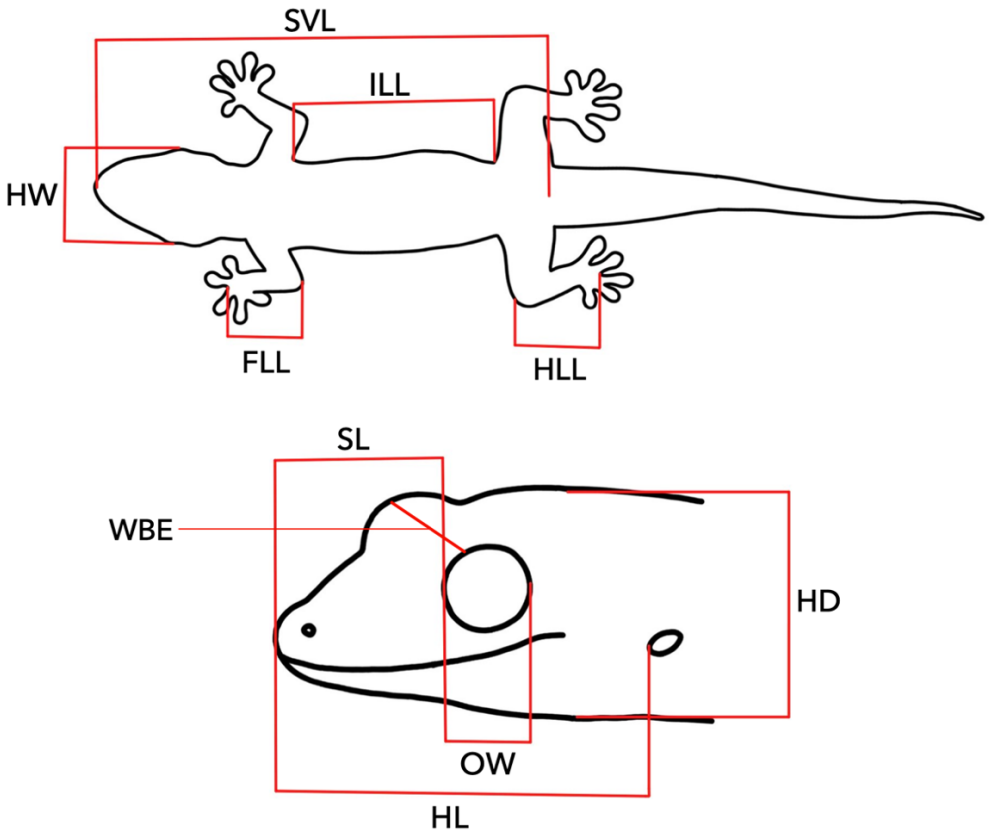

Figure S2. Morphological traits measured in this study. Traits and abbreviations are as follows: snout-to-vent length (SVL); head width (HW); inter-limb length (ILL); forelimb length (FLL); hindlimb length (HLL); snout length (SL); width-between-eyes (WBE); orbit width (OW); head depth (HD); head length (HL).

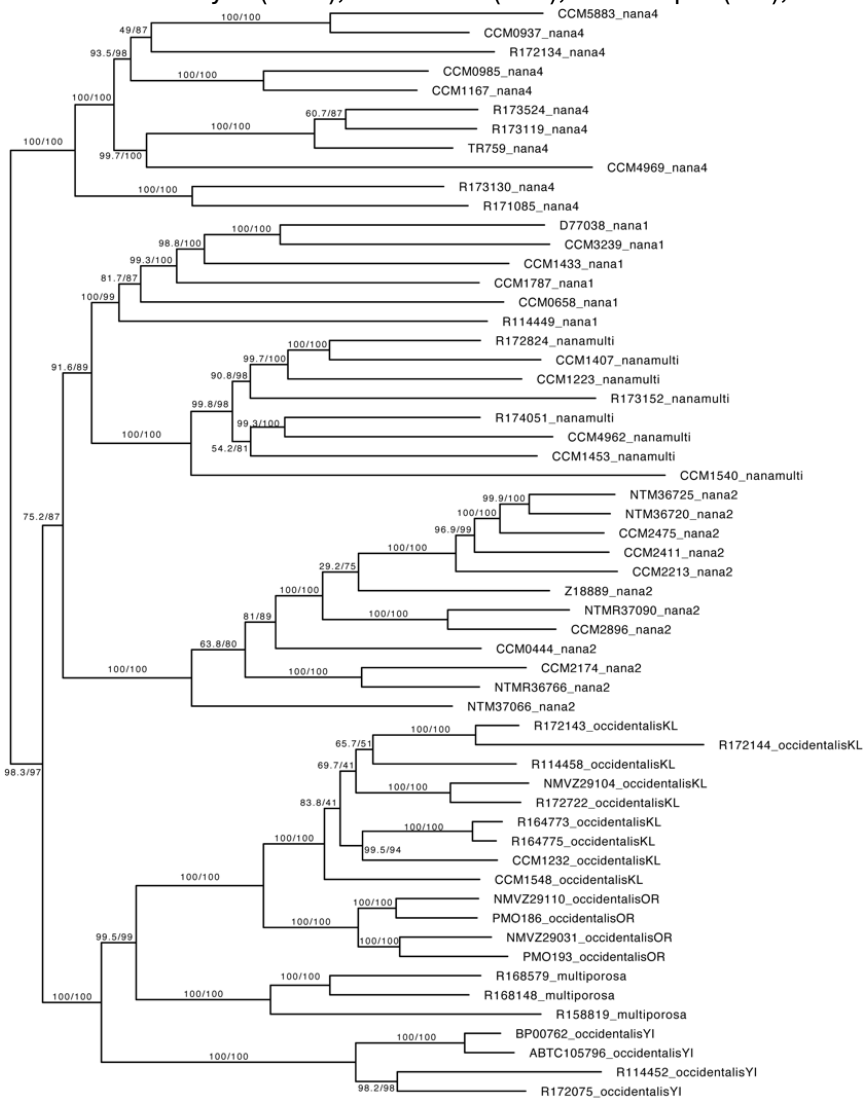

Figure S3. Phylogeny of the *Gehyra nana-occidentalis* group inferred from a concatenated alignment of 1,478 exons using IQ-TREE. Numbers on branches indicate SH-like aLRT / ultrafast bootstrap (UFB) support.

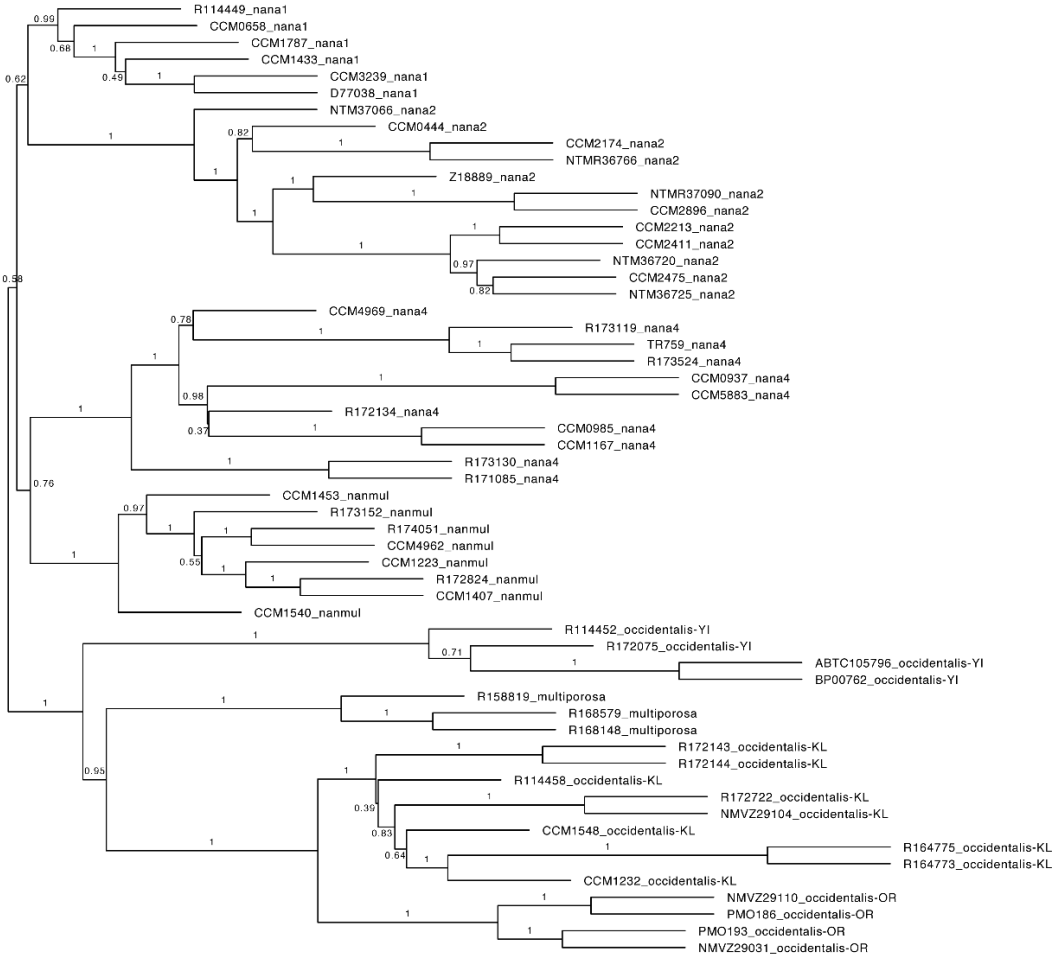

Figure S4. Phylogeny of the *Gehyra nana-occidentalis* group inferred from 1,478 gene trees using ASTRAL-III. Branches on gene trees with bootstrap support < 30 were collapsed. Numbers on branches indicate posterior probabilities.

Figure S5. Mitochondrial phylogeny of the *Gehyra nana-occidentalis* group inferred from 1,038 bp of the ND2 locus using IQ-TREE. Lineages are collapsed for graphical purposes where possible. Numbers on branches indicate ultrafast bootstrap (UFB) support.

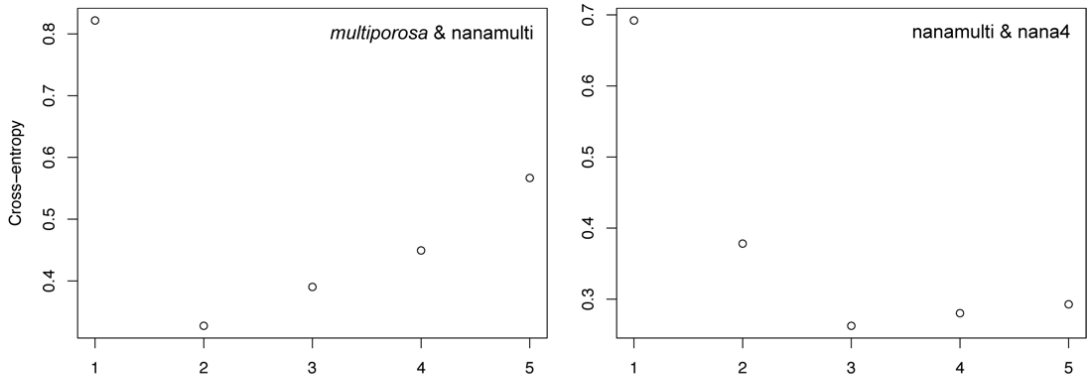

Figure S6. Cross entropy (ce) scores from sNMF for K = 1–5 at the two contact zones.

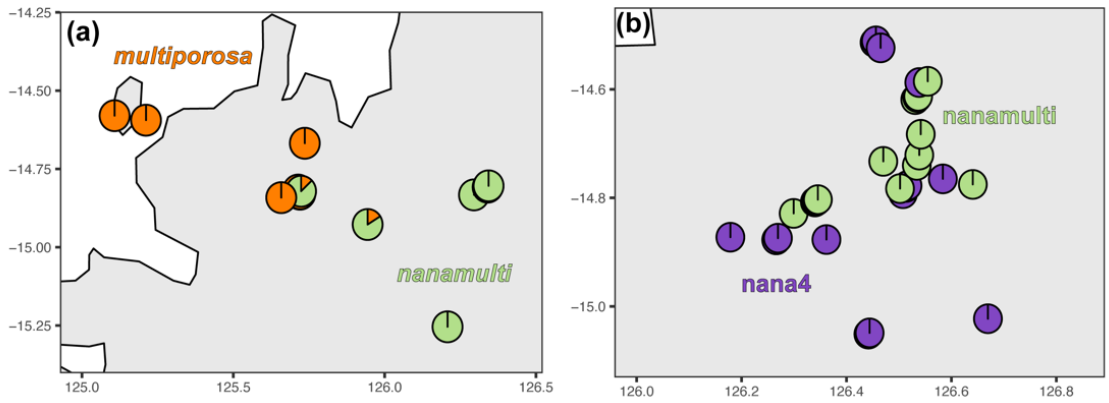

Figure S7. Maps each show pie charts that reflect individual admixture proportions estimated by sNMF at K = 2 at the two contact zones.

Table S1. Exon capture samples for the *Gehyra nana-occidentalis* group used in phylogenomics and introgression analyses. The 'Missing data' column shows the percentage of missing data for each sample for the 1,478 exonic loci dataset. The 'IQ-TREE + ASTRAL' column indicates whether the sample was used in the IQ-TREE and ASTRAL phylogenomic analyses, with samples excluded from these and subsequent analyses if they had excessively high missing data (≥ 40%) or else dubious locality data. The 'BPP Phylo' column indicates whether the sample was use in the BPP phylogenomics analysis and 'BPP MSCi' indicates whether the sample was used in at least one of the MSCi analyses.

Sample ID	Lineage	Missing data (%)	IQ-TREE + ASTRAL	BPP Phylo	BPP MSCi	Latitude	Longitude	Notes
CCM1217	*multiporosa*	61.45	No	No	No	-14.8317	125.7192	
R158819	*multiporosa*	1.02	Yes	Yes	Yes	-14.601944	125.203889	
R168148	*multiporosa*	2.09	Yes	Yes	Yes	-15.5944	125.1872	
R168579	*multiporosa*	1.23	Yes	Yes	Yes	-15.283333	124.383333	
CCM0534	nana1	41.2	No	No	No	-15.61091	131.11597	
CCM0658	nana1	1.89	Yes	Yes	No	-15.75056	129.08692	
CCM1433	nana1	4	Yes	No	No	-17.52945	126.20999	
CCM1787	nana1	1.96	Yes	Yes	No	-17.66931	128.30934	
CCM3239	nana1	9.46	Yes	No	No	-18.3272	125.765	
D77007	nana1	39.9	No	No	No	-17.14182	125.23882	
D77038	nana1	2.21	Yes	Yes	No	-18.75114	126.08203	
R114449	nana1	2.23	Yes	Yes	No	-16.15	123.75	
CCM0444	nana2	1.85	Yes	Yes	No	-14.43816	132.28014	
CCM2174	nana2	0.86	Yes	Yes	No	-14.71124	134.28859	
CCM2213	nana2	1.82	Yes	No	No	-14.76098	134.68181	
CCM2411	nana2	1.96	Yes	No	No	-14.65498	134.7812	
CCM2475	nana2	2.09	Yes	No	No	-14.27311	135.06345	
CCM2896	nana2	1.67	Yes	No	No	-13.11446	130.79838	
CCM3548	nana2	46.39	No	No	No	-14.219667	132.040333	
CCM3550	nana2	65.62	No	No	No	-14.219667	132.040333	
NTM36720	nana2	6.37	Yes	No	No	-14.178	134.364	
NTM36725	nana2	1.26	Yes	No	No	-14.089333	134.571833	
NTM37066	nana2	12.39	Yes	No	No	-14.814117	131.918833	
NTMR36766	nana2	3.81	Yes	No	No	-14.132833	134.343	
NTMR37090	nana2	14.65	Yes	Yes	No	-13.285067	131.117433	
Z18889	nana2	1.33	Yes	Yes	No	-12.188333	133.8125	
CCM0937	nana4	1.67	Yes	No	No	-14.52463	126.46395	
CCM0985	nana4	0.89	Yes	Yes	Yes	-14.88	126.35853	
CCM1167	nana4	6.58	Yes	Yes	Yes	-14.7699	126.5788	
CCM4969	nana4	3.79	Yes	No	No	-14.349779	127.750982	
CCM5883	nana4	3.48	Yes	No	No	-14.595349	126.541894	
R171085	nana4	9.48	Yes	No	No	-15.078056	128.141389	
R172134	nana4	3.52	Yes	No	No	-13.9391	126.1744	
R173119	nana4	7.31	Yes	No	No	-14.60824	126.93479	
R173130	nana4	0.76	Yes	Yes	Yes	-15.81666	128.09793	
R173524	nana4	1.90	Yes	No	No	-14.60824	126.93172	

Sample ID	Lineage	Missing data (%)	IQ-TREE + ASTRAL	BPP Phylo	BPP MSCi	Latitude	Longitude	Notes
TR759	nana4	1.46	Yes	Yes	Yes	-15.0053	126.83661	
CCM1182	nanamulti	1.2	No	Yes	Yes	-14.8237	125.7213	Dubious locality data.
CCM1223	nanamulti	1.17	Yes	Yes	Yes	-14.8237	125.7213	
CCM1407	nanamulti	22.54	Yes	No	No	-16.49599	125.3393	
CCM1453	nanamulti	11.06	Yes	No	No	-17.29092	127.25687	
CCM1540	nanamulti	21.34	Yes	No	No	-16.81862	126.22401	
CCM4962	nanamulti	1.99	Yes	Yes	No	-14.49111	127.65298	
R172824	nanamulti	2.67	Yes	No	No	-16.6575	125.929167	
R173152	nanamulti	2.34	Yes	Yes	Yes	-14.58944	126.55067	
R174051	nanamulti	1.68	yes	No	Yes	-14.77614	127.09767	
CCM1232	occidentalis-KL	1.94	Yes	Yes	Yes	-17.04067	125.2268	
CCM1548	occidentalis-KL	1.23	Yes	Yes	Yes	-16.81862	126.22401	
NMVZ29104	occidentalis-KL	2.27	Yes	No	No	-17.48246	125.02902	
R114458	occidentalis-KL	1.93	Yes	No	No	-16.083333	123.416667	
R146018	occidentalis-KL	6.79	No	No	No	-16.6833	123.8333	Dubious locality data.
R164773	occidentalis-KL	1.52	Yes	No	No	-16.7452	128.2825	
R164775	occidentalis-KL	0.92	Yes	Yes	Yes	-16.745278	128.2825	
R172143	occidentalis-KL	0.93	Yes	No	Yes	-16.0816	124.0706	
R172144	occidentalis-KL	7.18	Yes	No	No	-16.0925	124.0931	
R172722	occidentalis-KL	0.57	Yes	Yes	Yes	-17.408333	124.946111	
NMVZ29031	occidentalis-OR	1.17	Yes	Yes	Yes	-17.91662	125.3024	
NMVZ29110	occidentalis-OR	1.6	Yes	Yes	Yes	-17.558272	125.098489	
PMO186	occidentalis-OR	2	Yes	Yes	Yes	-17.6748	125.0704	
PMO193	occidentalis-OR	3.87	Yes	Yes	Yes	-18.02674	125.54425	
ABTC105796	occidentalis-YI	1.2	Yes	Yes	No	-16.429167	123.178611	
BP00762	occidentalis-YI	1.78	Yes	Yes	Yes	-16.43	123.18	
R114452	occidentalis-YI	4.46	Yes	Yes	Yes	-16.15	123.7833	
R165445	occidentalis-YI	80.58	No	No	No	-16.083889	123.541944	
R172075	occidentalis-YI	2.31	Yes	Yes	Yes	-16.622778	123.470833	
ABTC29238	paranana	35.03	No	No	No	-13.73	130.73	
CCM0651	paranana	0.46	No	No	No	-15.65862	129.65944	
CCM0652	paranana	19.12	No	No	No	-15.65862	129.65944	
CCM2881	paranana	27.14	No	No	No	-13.19654	130.71394	
CCM2936	paranana	1.51	Yes	No	No	-13.12641	130.80463	
NTM37056	paranana	78.02	No	No	No	-13.35	131.138	

Table S2. Samples for which we obtained genome-wide SNP data via DArTseq, their respective lineage, latitude, longitude, whether they were an early generation hybrid, and the contact zone they were included in (if applicable).

Sample ID	Lineage	Latitude	Longitude	Early gen hybrid?	Contact zone
CCM1185	*multiporosa*	-14.8317	125.7192		multiporosa/nanamulti
CCM1186	*multiporosa*	-14.8317	125.7192		multiporosa/nanamulti
CCM1211	*multiporosa*	-14.6723	125.7319		multiporosa/nanamulti
CCM1215	*multiporosa*	-14.8317	125.7192		multiporosa/nanamulti
CCM1217	*multiporosa*	-14.8317	125.7192		multiporosa/nanamulti
CCM2820	*multiporosa*	-14.82168	125.70993		multiporosa/nanamulti
R168148	*multiporosa*	-15.5944	125.1872		
WAMR158819	*multiporosa*	-14.601944	125.20389		multiporosa/nanamulti
WAMR158824	*multiporosa*	-14.601944	125.20389		multiporosa/nanamulti
WAMR168575	*multiporosa*	-15.35	124.53333		
WAMR168576	*multiporosa*	-15.35	124.53333		
WAMR168579	*multiporosa*	-15.283333	124.38333		
WAMR168585	*multiporosa*	-15.351	125.001		
WAMR168905	*multiporosa*	-14.585556	125.10222		multiporosa/nanamulti
WAMR171078	*multiporosa*	-15.026944	124.95389		
ABTC118947	nana1	-16.634715	129.33521		
CCM0534	nana1	-15.61091	131.11597		
CCM0658	nana1	-15.75056	129.08692		
CCM1433	nana1	-17.52945	126.20999		
CCM1489	nana1	-17.13767	125.07829		

Sample ID	Lineage	Latitude	Longitude	Early gen hybrid?	Contact zone
CCM1787	nana1	-17.66931	128.30934		
CCM1803	nana1	-17.64743	127.69274		
CCM2716	nana1	-15.645	130.4959		
CCM2720	nana1	-15.9354	129.6105		
CCM2723	nana1	-15.7652	128.7402		
CCM2808	nana1	-16.11707	128.73813		
CCM2951	nana1	-15.87227	130.32527		
CCM2984	nana1	-16.45158	130.10257		
CCM2998	nana1	-16.31998	130.44366		
CCM3015	nana1	-17.51892	129.87592		
CCM3033	nana1	-18.42522	127.81967		
CCM3079	nana1	-16.74565	128.28288		
CCM3095	nana1	-17.33473	128.38443		
CCM3239	nana1	-18.3272	125.765		
CCM3427	nana1	-15.76313	128.75131		
CCM5416	nana1	-16.8	130.26667		
CCM7265	nana1	-16.57263	128.33977		
CCM7283	nana1	-16.66349	128.52646		
CCM7305	nana1	-16.7632	128.27444		
CCM7469	nana1	-16.60579	128.95433		
CCM7867	nana1	-15.6586	129.659		
CCM7868	nana1	-15.6586	129.659		
CCM8043	nana1	-17.9025	127.8313		
CCM8044	nana1	-17.9025	127.8313		
D76950	nana1	-17.90913	125.28525		
D77007	nana1	-17.14182	125.23882		
D77035	nana1	-18.75114	126.08203		
D77042	nana1	-18.73955	125.96368		
PMO172	nana1	-17.6773	125.0889		
R37204	nana1	-15.95	131.06667		
R37597	nana1	-15.034267	129.86512		
R37691	nana1	-15.025467	130.47731		
R37720	nana1	-15.283	130.83212		
SMZ1634	nana1	-15.5519	130.9186		
SMZ1635	nana1	-15.5519	130.9186		
SMZ1644	nana1	-15.5431	130.95		
SMZ1661	nana1	-15.7487	130.6251		
SMZ1713	nana1	-15.9903	128.9711		
SMZ1761	nana1	-16.7463	128.2812		
SMZ1905	nana1	-17.9148	125.2991		
SMZ1952	nana1	-18.7366	126.0944		
SMZ1964	nana1	-17.483	128.3807		
SMZ1965	nana1	-17.483	128.3807		
SMZ1966	nana1	-17.483	128.3807		
SMZ1967	nana1	-17.483	128.3807		
SMZ2829	nana1	-15.7941	128.69		
SMZ2830	nana1	-15.7941	128.69		
SMZ2834	nana1	-16.1231	128.7375		
SMZ2839	nana1	-16.0363	128.8182		
SMZ2841	nana1	-15.9833	128.9463		
SMZ2845	nana1	-16.2268	128.3442		
SMZ2847	nana1	-16.1831	128.3805		
SMZ2855	nana1	-15.8575	128.8017		
SMZ2856	nana1	-15.8575	128.8017		
SMZ2857	nana1	-15.5148	128.835		
SMZ2859	nana1	-15.7314	128.7399		
SMZ2872	nana1	-16.5734	128.1992		
SMZ2886	nana1	-15.8721	129.0511		
SMZ2917	nana1	-15.5996	131.208		
SMZ2922	nana1	-15.6057	131.0795		
SMZ3019	nana1	-17.5045	126.1106		
SMZ3038	nana1	-17.5297	126.2131		
WAMR114449	nana1	-16.15	123.75		
ABTC112801	nana4	-13.939167	126.17444		

Sample ID	Lineage	Latitude	Longitude	Early gen hybrid?	Contact zone
BP02484	nana4	-14.486407	127.81917		
CCM0727	nana4	-15.1998	126.0874		multiporosa/nanamulti
CCM0921	nana4	-14.52463	126.46395		nana4/nanamulti
CCM0986	nana4	-14.88	126.35853		multiporosa/nanamulti
CCM1167	nana4	-14.7699	126.5788		nana4/nanamulti
CCM1665	nana4	-15.72028	127.81917		
CCM1751	nana4	-14.8791	126.172		multiporosa/nanamulti
CCM4968	nana4	-14.349779	127.75098		
CCM4971	nana4	-14.79563	127.93694		
CCM5883	nana4	-14.595349	126.54189		nana4/nanamulti
CCM7444	nana4	-15.53519	128.71225		
CCM7448	nana4	-15.17884	128.63002		
CCM7964	nana4	-14.7826	126.5112		nana4/nanamulti
CCM7965	nana4	-14.782806	126.51103		nana4/nanamulti
CCM7966	nana4	-14.782806	126.51103		nana4/nanamulti
CCM7967	nana4	-14.7826	126.5112		nana4/nanamulti
CCM7968	nana4	-14.7826	126.5112		nana4/nanamulti
CCM8005	nana4	-14.5885	126.5376		nana4/nanamulti
CCM8053	nana4	-15.8039	128.5048		
CCM8054	nana4	-15.8039	128.5048		
CMWA69	nana4	-15.90715	128.12544		
R173130	nana4	-15.81666	128.09793		
R174186	nana4	-14.5178	126.4489		nana4/nanamulti
R174189	nana4	-14.51675	126.45035		nana4/nanamulti
SMZ1501	nana4	-15.803	128.5066		
SMZ1723	nana4	-15.7144	128.2555		
SMZ1724	nana4	-15.7144	128.2555		
SMZ1725	nana4	-15.86455	128.38844		
SMZ1726	nana4	-15.864262	128.38949		
SMZ1763	nana4	-15.9698	128.4202		
SMZ1772	nana4	-15.782875	128.55258		
SMZ1773	nana4	-15.770748	128.6183		
SMZ1774	nana4	-15.7707	128.6183		
SMZ1776	nana4	-15.770217	128.61919		
SMZ1796	nana4	-14.881707	126.26184		multiporosa/nanamulti
SMZ1797	nana4	-14.8817	126.2618		multiporosa/nanamulti
SMZ1798	nana4	-14.8817	126.2618		multiporosa/nanamulti
SMZ1820	nana4	-14.5884	126.5375		nana4/nanamulti
SMZ1821	nana4	-14.5884	126.5375		nana4/nanamulti
SMZ1822	nana4	-14.5884	126.5375		nana4/nanamulti
SMZ1823	nana4	-14.5884	126.5375		nana4/nanamulti
SMZ1877	nana4	-14.783062	126.51078		nana4/nanamulti
SMZ1878	nana4	-14.782762	126.51114		nana4/nanamulti
SMZ1879	nana4	-14.7837	126.5098		nana4/nanamulti
SMZ2828	nana4	-15.7871	128.6792		
SMZ2843	nana4	-16.3598	128.225		
SMZ2849	nana4	-16.1113	128.3818		
SMZ2851	nana4	-16.0617	128.4062		
SMZ2884	nana4	-15.7674	128.6523		
SMZ3000	nana4	-16.0143	128.0137		
SMZ3006	nana4	-16.0127	127.9768		
TR758	nana4	-15.01073	126.83552	nanamulti/nana4	
TS1614	nana4	-15.056383	126.43642		multiporosa/nanamulti
TS1615	nana4	-15.056383	126.43642		multiporosa/nanamulti
WAMR172336	nana4	-14.8	126.5		nana4/nanamulti
WAMR172912	nana4	-15.1324	126.1474		multiporosa/nanamulti
WAMR173119	nana4	-14.60824	126.93479		
WAMR174107	nana4	-15.02725	126.66505		
ABTC137453	nanamulti	-16.44338	127.78315		
BP02238	nanamulti	-14.740131	128.30336		
CCM0764	nanamulti	-15.3522	126.5899		
CCM0880	nanamulti	-14.83431	126.29359		multiporosa/nanamulti
CCM1017	nanamulti	-16.0969	126.5112		
CCM1065	nanamulti	-15.2609	126.201		multiporosa/nanamulti

Sample ID	Lineage	Latitude	Longitude	Early gen hybrid?	Contact zone
CCM1160	nanamulti	-14.7811	126.6349		nana4/nanamulti
CCM1223	nanamulti	-14.8237	125.7213		multiporosa/nanamulti
CCM1407	nanamulti	-16.49599	125.3393		
CCM1453	nanamulti	-17.29092	127.25687		
CCM1501	nanamulti	-16.90368	125.7606		
CCM1538	nanamulti	-16.81862	126.22401		
CCM1546	nanamulti	-16.81862	126.22401		
CCM1571	nanamulti	-16.53559	126.12857		
CCM1573	nanamulti	-16.53559	126.12857		
CCM1600	nanamulti	-16.49046	126.21177		
CCM1626	nanamulti	-16.17108	125.98763		
CCM4962	nanamulti	-14.49111	127.65298		
CCM7969	nanamulti	-14.7892	126.4957		nana4/nanamulti
CCM8004	nanamulti	-14.5947	126.5438		nana4/nanamulti
CCM8041	nanamulti	-15.9377	127.2216		
CCM8042	nanamulti	-15.9377	127.2216		
MCZA28615	nanamulti	-14.58944	126.55067		nana4/nanamulti
R172825	nanamulti	-16.6575	125.92917		
R174051	nanamulti	-14.77614	127.09767		
SMZ1499	nanamulti	-14.9336	125.9376		multiporosa/nanamulti
SMZ1807	nanamulti	-14.811018	126.33762		multiporosa/nanamulti
SMZ1808	nanamulti	-14.810548	126.3367		multiporosa/nanamulti
SMZ1809	nanamulti	-14.811297	126.33703		multiporosa/nanamulti
SMZ1810	nanamulti	-14.811301	126.3371		multiporosa/nanamulti
SMZ1837	nanamulti	-14.594393	126.54423		nana4/nanamulti
SMZ1838	nanamulti	-14.59335	126.54457		nana4/nanamulti
SMZ1839	nanamulti	-14.593392	126.54453		nana4/nanamulti
SMZ1840	nanamulti	-14.594937	126.54378		nana4/nanamulti
SMZ1847	nanamulti	-14.619821	126.52953		nana4/nanamulti
SMZ1848	nanamulti	-14.620619	126.52931		nana4/nanamulti
SMZ1849	nanamulti	-14.6206	126.5293		nana4/nanamulti
SMZ1855	nanamulti	-14.690829	126.53347		nana4/nanamulti
SMZ1858	nanamulti	-14.723562	126.5363		nana4/nanamulti
SMZ1860	nanamulti	-14.743422	126.53065		nana4/nanamulti
TS1606	nanamulti	-14.73675	126.4661		nana4/nanamulti
WAMR172831	nanamulti	-15.957778	127.0625		
CCM1293	occidentalis-KL	-16.78657	124.92196		
CCM1303	occidentalis-KL	-16.97111	125.02998		
CCM1337	occidentalis-KL	-17.11856	125.13182		
CCM1374	occidentalis-KL	-16.49954	125.33637		
CCM1439	occidentalis-KL	-17.52933	126.21127		
CCM1493	occidentalis-KL	-17.16653	125.34761		
CCM1548	occidentalis-KL	-16.81862	126.22401		
CCM1566	occidentalis-KL	-16.53559	126.12857		
CCM1670	occidentalis-KL	-16.34058	126.24382		
CCM7366	occidentalis-KL	-17.17496	125.29897		
CCM7625	occidentalis-KL	-16.74726	128.28123		
CCM7628	occidentalis-KL	-16.74726	128.28123		
CCM7630	occidentalis-KL	-16.74726	128.28123		
CCM8073	occidentalis-KL	-16.6558	125.9256		
CCM8074	occidentalis-KL	-16.6558	125.9256		
CCM8075	occidentalis-KL	-16.6558	125.9256		
PMO174	occidentalis-KL	-17.47945	125.02886		
R172143	occidentalis-KL	-16.0816	124.0706		
R172144	occidentalis-KL	-16.0925	124.0931		
R172724	occidentalis-KL	-17.408333	124.94611		
R172731	occidentalis-KL	-17.432222	124.98083		
R172797	occidentalis-KL	-17.432222	124.98083		
R172798	occidentalis-KL	-17.34001	124.8242		
SMZ3016	occidentalis-KL	-17.5045	126.1106		
SMZ3020	occidentalis-KL	-17.5293	126.2121		
WAMR171593	occidentalis-KL	-15.976944	125.36667		
CCM3311	occidentalis-OR	-18.1048	125.6919		
D76949	occidentalis-OR	-17.90913	125.28525		

Sample ID	Lineage	Latitude	Longitude	Early gen hybrid?	Contact zone
PMO181	occidentalis-OR	-17.69499	125.14423		
PMO186	occidentalis-OR	-17.6748	125.0704		
PMO203	occidentalis-OR	-18.1064	125.6899		
PMO207	occidentalis-OR	-18.02732	125.54452		
PMO212	occidentalis-OR	-18.0272	125.54402		
R172720	occidentalis-OR	-17.607778	125.14556		
SMZ3281	occidentalis-OR	-17.9149	125.2998		
WAMR172719	occidentalis-OR	-17.607778	125.14556		
R146018	occidentalis-YI	-16.6833	123.8333		
R165445	occidentalis-YI	-16.083889	123.54194		
R165551	occidentalis-YI	-16.141111	123.74861		
R168303	occidentalis-YI	-16.020119	123.51924		
R172076	occidentalis-YI	-16.254167	123.82444		
R172097	occidentalis-YI	-16.6225	123.47139		
CCM7831	*paranana*	-13.12576	130.80212		
CCM7832	*paranana*	-13.12576	130.80212		
CCM7834	*paranana*	-13.12576	130.80212		
CCM7836	*paranana*	-13.12576	130.80212		
CCM7864	*paranana*	-15.6586	129.659		
CCM7865	*paranana*	-15.6586	129.659		
CCM7866	*paranana*	-15.6586	129.659		
CDU375	*paranana*	-13.12468	130.7995		
CDU376	*paranana*	-13.12468	130.7995		
CDU378	*paranana*	-13.12468	130.7995		
CDU380	*paranana*	-13.12468	130.7995		
CDU546	*paranana*	-13.20427	130.7139		
R37601	*paranana*	-15.034267	129.86512		
SMZ2025	*paranana*	-13.2179	130.7355		
SMZ2026	*paranana*	-13.2179	130.7355		
SMZ2027	*paranana*	-13.2179	130.7355		

Table S3. Information for the four contact zones examined herein.

Lineage 1	Lineage 2	Variant sites	Latitude	Longitude	Radius
nanamulti	nana4	2,192	-14.80102	126.48523	40 km
multiporosa	nanamulti	1,828	-14.95255	125.74066	80 km

Table S4. Samples used in analyses of morphological data. Sample ID numbers all represent WAM R accession numbers. Columns 4–13 represent linear morphometric variables in mm, abbreviations for which are as follows: SVL, snout-to-vent length; HL, head length; HD, head depth; HW, head width; SL, snout length; OW, orbit width; WBE, width-between-eyes; ILL, interlimb length; HLL, hindlimb length; FLL, forelimb length.

Sample ID	Sex	Lineage	SVL	HL	HD	HW	SL	OW	WBE	ILL	HLL	FLL
167804	m	multiporosa	49.99	11.58	5.5	9.75	5.11	3.53	3.54	21.44	7.33	6.24
171491	m	multiporosa	53.24	12.58	5.76	10.6	5.53	3.82	3.77	22.91	7.4	6.3
168577	m	multiporosa	52.15	12.35	5.24	10.12	5.1	3.55	3.7	21.39	7.19	6.45
168584	f	multiporosa	53.77	12.38	5.48	10.27	5.5	3.81	3.94	22.69	7.23	6.4
168177	f	multiporosa	55.28	12.85	5.49	10.13	5.62	3.77	3.9	24.28	7.19	6.63
171547	f	multiporosa	47.46	11.88	4.7	9.59	5.06	3.48	3.57	20.45	7.01	6.16
168902	f	multiporosa	50.71	11.85	5.29	9.4	5.2	3.71	3.22	22.18	7.58	6.16
167855	m	multiporosa	48.98	11.83	5.39	9.39	5.13	3.52	3.23	21.75	7.58	6.57
96949	f	multiporosa	53.8	12.48	5.07	10.29	5.27	4.24	3.71	23.24	7.9	6.69
172066	m	multiporosa	51.98	12.32	5.49	10.15	5.21	4.12	3.64	23.66	7.26	6.31
168587	m	multiporosa	50.83	12.34	5.22	10.28	5.22	3.93	3.37	22.99	7.12	6.13
168711	f	multiporosa	53.45	12.45	5.19	10.23	5.49	4.03	3.25	23.28	7.2	6.35
158819	f	multiporosa	45.66	11.25	4.98	9.14	4.9	3.51	3.03	20.74	6.14	5.44
168582	m	multiporosa	50.52	12.34	4.96	9.31	5.28	3.49	3.05	22.6	7.04	5.95
168732	f	multiporosa	49.84	11.67	4.81	9.96	5.05	3.43	2.94	22.4	6.62	6.25
83711	m	occidentalis-KL	57.94	13.94	6.51	10.98	6.11	3.84	3.75	25.82	8.65	7.6
176207	f	occidentalis-KL	41.73	10.99	4.22	8.6	4.6	3.53	2.82	18.27	5.81	5.34
175756	m	occidentalis-KL	66.6	16.02	7.14	12.56	6.99	4.63	4.74	29.71	10.04	9.02
175752	m	occidentalis-KL	63.44	14.84	5.88	12.21	6.16	4.36	4.31	28.9	9.32	8.67
175764	f	occidentalis-KL	49.77	12.24	4.65	9.37	4.97	3.69	3.22	23.85	6.65	6.33

Sample ID	Sex	Lineage	SVL	HL	HD	HW	SL	OW	WBE	ILL	HLL	FLL
175760	m	occidentalis-KL	61.44	14.58	6.14	11.21	6.16	4.24	4.27	28.24	8.84	7.78
175755	m	occidentalis-KL	59.62	14.25	5.88	10.93	6.03	4.27	4.05	27.32	8.67	7.88
175761	f	occidentalis-KL	60.76	15.76	6.42	12.42	6.68	4.57	4.4	25.63	8.99	8.3
175753	f	occidentalis-KL	54.11	13.96	5.03	10.77	5.64	4.14	3.82	23.42	8.05	7.13
175757	m	occidentalis-KL	64.26	15.37	6.78	12.13	6.4	4.21	4.45	28.74	9.2	8.63
175762	f	occidentalis-KL	60.9	15.2	5.98	11.71	6.28	4.55	4.1	27.49	8.84	8.1
175490	f	occidentalis-KL	60.11	14.06	5.39	11.57	6.4	4.58	4.04	26.44	9.13	8.11
172798	f	occidentalis-KL	56.68	14.55	6.13	11.07	6.16	4.43	4.07	25.13	9.21	8.29
175758	f	occidentalis-KL	55.58	13.47	5.26	10.69	5.69	4.1	3.99	24.4	8.4	7.35
172768	m	occidentalis-KL	62.54	14.89	6.6	11.35	6.36	4.66	4.26	28.13	9.83	8.35
172826	f	occidentalis-KL	60.56	14.55	5.55	11.24	6.12	4.36	4.19	28.6	8.71	7.68
175482	m	occidentalis-KL	63.67	15.48	6.22	12.34	6.29	4.95	4.6	28.76	9.8	8.84
172778	f	occidentalis-KL	63.1	15.25	6.49	11.74	6.49	4.53	4.31	28.61	9.38	8.22
175479	m	occidentalis-KL	65.81	15.75	6.7	12.53	6.65	4.74	4.63	28.49	9.88	8.91
172786	m	occidentalis-KL	57.39	14.53	6.11	11.62	6.26	4.49	4.26	25.54	8.76	8.19
175488	f	occidentalis-KL	58.56	14.53	5.31	11.69	6.16	4.45	4.36	24.13	9.08	8.22
175481	f	occidentalis-KL	59.63	14.3	6.58	11.96	6.22	4.32	4.26	26.84	9.33	8.39
175497	f	occidentalis-KL	56.5	13.77	5.68	10.97	5.82	4.22	4.12	24.47	8.89	7.64
172785	f	occidentalis-KL	65.45	15.8	6.62	12.98	6.47	4.58	4.33	29.66	9.23	8.54
175483	m	occidentalis-KL	62	15.5	6.03	12.33	6.25	4.37	4.16	26.18	9.07	8.39
175494	f	occidentalis-KL	62.48	15.01	6.75	11.8	6.32	4.76	4.21	28.12	9.65	9.05
175491	m	occidentalis-KL	63.63	15.32	6.86	12.12	6.47	4.51	4.24	27.06	9.57	8.67
175498	m	occidentalis-KL	53.86	13.08	5.24	10.29	5.46	3.88	3.85	23.23	8.37	7.51
175499	f	occidentalis-KL	62.14	14.56	5.84	11.61	6.3	4.2	4.21	28.57	9.27	8.4
172797	f	occidentalis-KL	65.37	15.92	6.64	12.29	6.67	4.71	4.3	29.69	9.89	8.82
172799	m	occidentalis-KL	64.05	14.93	6.23	11.72	6.48	4.47	4.4	27.84	9.77	8.83
175487	f	occidentalis-KL	47.18	12.01	4.37	8.94	5.2	4	3.45	20.54	6.69	6.43
172732	m	occidentalis-KL	65.4	16.19	6.96	12.79	6.85	4.93	4.59	28.98	10.07	9.58
172722	f	occidentalis-KL	64.51	15.97	6.56	12.64	6.67	4.78	4.39	28.74	10.25	9.1
172724	f	occidentalis-KL	58.86	15.52	6.65	11.71	6.32	4.52	4.24	26.97	9.53	9.11
172731	f	occidentalis-KL	59.26	14.89	6.11	11.26	6.16	4.8	3.91	28.37	9.3	8.6
172730	f	occidentalis-KL	64.6	16.01	7.08	12.05	6.79	4.84	4.3	28.08	9.78	9.13
172723	f	occidentalis-KL	59.08	14.71	6	11.15	6.32	4.46	4.14	26.02	9.23	8.48
172101	f	occidentalis-KL	60.52	15.32	6.64	11.94	6.3	4.76	4.38	26.94	9.63	8.79
172094	m	occidentalis-KL	62.66	15.31	6.34	11.81	6.51	4.68	4.44	28.63	8.89	8.3
172073	m	occidentalis-KL	57.18	14	6.6	11	5.83	4.33	4.18	26.53	8.53	7.32
168194	f	occidentalis-KL	60.6	14.33	5.91	11.05	6.23	5.05	4.34	26.35	8.81	8.38
164775	f	occidentalis-KL	75.13	17.96	7.52	12.97	7.78	5.42	4.73	33.88	11.93	10.78
164774	f	occidentalis-KL	66.79	16.9	6.86	12.72	7.17	4.91	4.54	29.32	10.84	10
164773	f	occidentalis-KL	62.73	15.43	6.34	11.59	6.57	4.59	4.31	28	9.8	9.02
172728	f	occidentalis-OR	55.97	13.88	6.13	10.39	5.9	4.29	3.93	25.09	8.93	8.13
172719	m	occidentalis-OR	60.87	14.99	6.32	11.29	6.17	4.68	4.18	27.02	9.3	8.36
172718	f	occidentalis-OR	56.56	13.28	5.75	10.56	5.22	4.21	3.77	24.28	8.29	7.19
172077	f	occidentalis-OR	54.53	13.76	5.57	9.64	5.67	4.3	3.72	23.38	8.33	7.71
172074	f	occidentalis-OR	63.17	15.39	6.39	11.74	6.7	4.44	4.21	27.71	9.69	8.83
172076	m	occidentalis-YI	63.22	15.57	7.11	13.03	6.46	4.7	4.56	28.54	8.73	7.81
172097	f	occidentalis-YI	55.65	13.98	6.01	10.57	5.85	4.27	4.15	25.38	7.85	6.98
172086	f	occidentalis-YI	60.09	14.96	6.52	12.29	6.33	5.07	4.46	27.61	8.69	7.85
172075	f	occidentalis-YI	61.08	14.73	6.4	11.62	6.14	4.8	4.3	28.53	8.51	7.57
165445	f	occidentalis-YI	56.92	13.73	4.76	11.29	5.89	4.32	4.15	25.12	8.09	7.27
172104	m	occidentalis-YI	54.68	13.3	5.69	10.1	5.68	4.2	4.01	25.17	7.83	7.03
172708	m	occidentalis-YI	68.96	16.32	6.58	13.1	6.96	5.14	4.93	28.24	9.29	8.2
172078	m	occidentalis-YI	60.27	14.56	6.86	11.61	5.99	4.81	4.47	26.43	8.38	7.59
158009	f	occidentalis-YI	59.07	14.03	6.89	10.88	6.03	4.25	4.36	26.62	8.27	7.43
114453	f	occidentalis-YI	57.65	14.65	6.14	10.92	6.08	4.33	4.21	24.22	7.99	7.13
168249	f	occidentalis-YI	59.76	14.65	6.35	11.49	6.2	4.58	4.29	24.89	7.97	7.31
172100	m	occidentalis-YI	58.71	14.44	6.37	10.44	6.3	4.35	4.16	25.73	7.93	7.15
172082	f	occidentalis-YI	60.42	13.88	5.87	10.66	5.99	4.29	4.08	27.22	8.09	7.42
176248	m	nanamulti	47.1	12	4.79	9.04	5.07	3.52	3.5	20.33	6.8	5.9
176439	m	nanamulti	50.99	12.37	4.99	9.99	5.47	3.7	3.68	20.7	6.9	6.39
176446	f	nanamulti	44.18	10.92	4.28	8.58	4.56	3.3	3.4	19.58	5.9	5.62
176437	f	nanamulti	45.96	10.93	4.49	9.04	4.54	3.39	3.31	19.09	5.97	5.18
176444	f	nanamulti	44.21	10.56	3.72	8.19	4.5	3.18	3.26	17.7	5.98	5.87
176280	f	nanamulti	42.76	10.71	3.62	8.41	4.38	3.09	3.33	18.7	6.29	5.61
176438	f	nanamulti	40.67	10.41	3.96	8.66	4.2	3.37	3.2	16.73	6.05	5.12
176443	f	nanamulti	43.11	11.51	4.27	8.97	4.51	3.45	3.24	19.7	6.28	5.42
176442	f	nanamulti	44.49	10.89	3.87	9.36	4.56	3.32	3.35	18.42	6.35	5.26
176450	m	nanamulti	38.89	9.71	3.88	7.4	3.78	2.95	2.92	17.89	5.8	5
176268	m	nanamulti	46.21	11.66	4.62	9.49	4.86	3.6	3.42	19.6	6.56	5.36
176433	m	nanamulti	39.74	9.94	4.09	7.89	4.07	3.19	3.13	16.61	5.72	4.97
176434	m	nanamulti	43.86	10.82	4.68	8.4	4.32	3.45	3.24	19.67	6.4	5.66

Sample ID	Sex	Lineage	SVL	HL	HD	HW	SL	OW	WBE	ILL	HLL	FLL
176432	f	nanamulti	41.43	10.43	4	8.65	4.38	3.11	3.16	16.78	5.82	5.02
176441	m	nanamulti	44.07	11.01	4.62	8.37	4.55	3.46	3.22	18.21	6.39	5.56
176451	m	nanamulti	42.65	10.53	4.19	8.56	4.33	3.45	3.1	18.23	6.28	5.38
176454	m	nanamulti	37.65	9.76	3.87	7.32	3.97	2.89	2.8	15.89	5.6	4.78
176448	f	nanamulti	37.45	9.53	3.47	7.76	3.89	2.74	2.71	16.56	5.45	4.65
176453	f	nanamulti	39.6	10.46	4.35	7.72	4.28	3.32	2.94	15.87	5.93	5.21
176330	f	nanamulti	43.42	10.81	4.48	7.37	4.34	3.4	3.14	18.04	6.33	5.9
176198	f	nanamulti	42.51	10.35	3.86	7.73	4.32	3.61	3.06	18.8	5.91	5.04
176447	m	nanamulti	46.7	11.16	4.7	8.6	4.76	3.73	3.37	21.94	6.42	5.77
176452	f	nanamulti	35.14	8.93	3.69	7.01	3.73	2.7	2.83	14.6	5.05	4.54
174207	f	nanamulti	41.97	10.67	4.95	8.21	4.33	3.14	3.03	17.76	6.3	5.42
174051	f	nanamulti	39.1	9.39	3.39	7.8	4.04	3.09	2.86	16.71	5.89	5.01
174050	f	nanamulti	43.47	10.69	4.62	8.52	4.5	3.38	3.21	19.86	6.62	5.7
172830	m	nanamulti	41.65	10.76	3.95	8.03	4.49	3.19	3.13	17.73	5.87	5.21
173150	m	nanamulti	38.49	9.17	4.12	7.06	3.95	2.96	3.02	16.86	5.74	5.09
173147	f	nanamulti	39.13	9.52	4.04	7.31	3.92	3.06	2.99	16.54	5.66	5.01
173152	m	nanamulti	38.99	9.92	4.54	7.83	4.13	3.2	2.91	15.96	5.78	5.28
172831	m	nanamulti	43.69	11.09	4.23	8.39	4.68	3.45	3.29	17.56	6.01	5.28
172824	f	nanamulti	41.77	10.23	4.28	8.18	4.37	3.42	3.12	17	6.18	5.47
172825	f	nanamulti	45.53	11.21	4.6	8.98	4.83	3.38	3.36	18.8	6.69	5.58
172832	m	nanamulti	41.53	10.52	4.09	7.59	4.29	3.24	3.1	17.3	6.06	5.37
173146	m	nanamulti	40.56	9.54	4.15	7.66	4.04	3.13	3.05	17.33	5.64	5.1
172875	f	nanamulti	39.55	9.89	3.89	7.41	4.15	3.4	2.97	16	5.85	5.2
113968	m	nanamulti	41.31	10.49	4.2	8.06	4.16	3.09	3.08	16.43	5.81	5.01
28214	m	nana4	48.65	12.25	5.68	9.89	5.26	3.4	3.26	22.03	7.89	7.02
179820	f	nana4	55.99	14.58	5.59	11.2	6.18	4.12	3.86	23.64	8.1	7.08
176164	m	nana4	47.97	12.29	4.89	9.32	5.25	3.52	3.16	20.99	7.65	6.46
176334	f	nana4	46.03	11.72	3.7	9.26	4.89	3.48	3.34	20.11	6.65	6
176187	f	nana4	38.62	9.96	3.96	7.24	4.28	3.18	3.05	15.38	5.67	4.63
176186	f	nana4	40.55	10.06	3.48	7.27	4.2	3.2	3.03	17.66	5.51	4.89
176188	f	nana4	48.59	12.36	4.84	9.45	5.28	3.95	3.42	19.83	6.9	6.18
176172	f	nana4	40.86	10.19	3.64	7.82	4.47	3.21	3.1	16.42	6.06	5.47
176199	f	nana4	50.64	12.23	4.83	8.65	5.41	3.93	3.16	21.63	6.87	6.27
176340	m	nana4	42.2	10.6	4.15	8.32	4.53	3.26	3.2	17.42	5.84	5.04
176337	m	nana4	39.97	10.04	3.92	7.67	4.23	3.1	3.17	17.28	5.86	5.14
176275	m	nana4	50.59	11.9	4.78	9.19	5.25	3.8	3.51	22.45	7.38	6.31
176333	m	nana4	44.97	11.09	4.36	8.77	4.73	3.44	3.3	20.09	6.76	5.98
176200	m	nana4	49.48	12.16	5.07	9.76	5.18	3.79	3.37	21.29	7.14	6.75
176338	f	nana4	45.31	11.43	4.76	8.18	4.69	3.57	3.54	19.66	6.53	5.51
176276	f	nana4	38.36	9.6	3.57	7.65	4.07	3.09	2.88	15.02	5.78	4.88
174107	m	nana4	46.5	11.54	4.57	8.51	5.05	3.6	3.19	21.57	6.65	6.29
174105	f	nana4	46.61	11.33	4.87	8.43	4.93	3.52	3.3	20.69	6.61	5.94
174189	m	nana4	45.58	10.89	4.47	8.56	4.67	3.45	3.42	19.1	6.36	5.73
172174	m	nana4	46.04	11.06	3.86	8.94	4.78	3.78	3.51	20.16	6.45	5.86
171086	m	nana4	47.17	11.58	4.69	8.63	4.92	3.54	3.56	20.38	6.35	5.82
171090	f	nana4	36.09	9.34	4.03	7.14	3.96	2.94	2.8	14.23	5.18	4.63
173128	m	nana4	43.15	10.9	4.73	8.49	4.54	3.49	3.24	18.21	6.19	5.58
172336	m	nana4	47.17	11.94	4.78	9.22	5.19	3.82	3.51	19.27	6.61	5.89
173524	f	nana4	39.05	9.71	3.57	7.03	4	2.93	2.96	17.06	5.7	5.19
171089	f	nana4	45.33	11.71	4.45	8.55	4.86	3.56	3.42	18.3	6.66	6.2
173129	f	nana4	42.26	10.92	4.57	8.84	4.49	3.17	3.25	17.75	6.26	5.8
172134	f	nana4	39.94	9.97	4.12	7.77	4.05	2.92	3.08	16.74	5.58	5.08
173130	m	nana4	38.22	9.86	4.13	7.56	4	3	3.03	15.29	5.76	5.29
173119	f	nana4	46.55	11.21	4.83	8.76	4.58	3.43	3.41	21.38	6.67	6.08
172135	f	nana4	39.46	10.13	4.21	7.76	4.16	3	3.07	16.19	5.76	5.42
151871	f	nana4	46.62	11.32	4.79	9.11	4.65	3.41	3.37	20.79	6.5	5.44
162518	m	nana4	47	11.67	4.65	8.59	4.81	3.36	3.17	20.57	6.69	5.89
151965	m	nana4	48.44	11.94	5.15	9.73	4.9	3.67	3.51	20.66	6.97	6.19
152015	m	nana4	49.59	11.74	5.03	9.36	4.98	3.68	3.47	21.25	7.03	6.3
151966	f	nana4	49.23	11.84	5.36	9.21	4.93	3.6	3.63	22.31	6.73	6.14
164853	m	nana4	46.72	11.54	4.64	9.25	4.97	3.47	3.37	19.94	6.38	5.79
151961	m	nana4	47.68	11.35	4.93	8.51	4.82	3.64	3.52	19.93	6.75	6.11
161187	m	nana4	45.4	11.29	5.03	8.87	4.74	3.36	3.4	19.11	6.47	6
117999	f	nana4	38.55	10.05	4.12	7.81	4.13	3.04	2.94	16.22	5.68	5.1
113991	m	nana4	39.07	10.28	4.32	7.92	4.35	3.09	3.1	15.53	5.9	5.56
117749	f	nana4	45.54	11.49	5	8.5	4.82	3.67	3.33	21.95	6.82	5.95
176223	f	nana1	42.22	10.12	3.81	7.52	4.26	3.28	3	19.57	6.15	5.69
176389	f	nana1	42.42	10.27	4.18	7.31	4.32	3.18	3.09	17.34	6.27	5.3
176301	m	nana1	39.37	9.41	3.33	7.34	4.04	3.01	2.87	16.52	5.93	5.01
175057	m	nana1	41.16	10.08	3.84	8.23	4.18	3.33	3.04	18.3	6.24	5.79
175061	m	nana1	36.56	9.46	3.74	7.31	3.88	3.02	2.78	16.4	5.78	5.14

Sample ID	Sex	Lineage	SVL	HL	HD	HW	SL	OW	WBE	ILL	HLL	FLL
175059	m	nana1	44.24	10.66	3.91	8.49	4.4	3.29	3.29	18.63	6.25	5.77
175053	m	nana1	42.18	10.53	4.21	8.21	4.44	3.28	3.24	18.45	6.19	5.71
175062	f	nana1	42.19	10.68	4.23	7.87	4.45	3.15	3.22	17.31	6.34	5.66
175058	m	nana1	42.16	10.07	3.56	8.37	3.98	3.11	3.24	17.32	6.17	5.73
175064	f	nana1	39.65	10	3.95	7.35	3.95	3.12	2.91	17.02	5.95	5.26
175060	m	nana1	41.14	9.91	3.72	7.66	4.08	3.27	2.89	17.07	6.08	5.62
175063	f	nana1	40.66	10.03	3.79	7.08	4.16	3.03	3.07	16.66	5.88	5.11
175052	f	nana1	41.06	9.7	3.78	7.49	4.14	3.15	3.02	18.41	6.09	5.56
174990	m	nana1	41.61	10.73	4.07	8.2	4.42	3.15	3.08	17.44	6.1	5.66
175050	m	nana1	37.77	9.36	3.84	7.36	3.89	2.89	2.73	16.19	5.66	4.98
132857	f	nana1	39.83	9.59	4.21	7.55	4.08	2.96	2.91	16.74	5.94	5.29
132858	f	nana1	40.42	10.07	3.9	7.6	4.3	3.22	2.96	17.38	6.07	5.34
165545	f	nana1	38.4	9.61	3.42	6.9	3.9	2.96	2.72	15.34	5.61	5.23
108735	f	nana1	40.51	9.68	3.99	7.61	4.31	2.97	2.98	18.46	5.88	5.33
125993	f	nana1	42.57	10.01	4.44	8.15	4.13	3.56	3.05	18.49	6.16	5.52
108733	m	nana1	40.27	9.8	4.2	7.6	4.11	2.99	2.94	16.25	5.7	5.22
108729	m	nana1	38.06	9.75	4.06	7.65	3.94	3	2.83	14.45	5.6	5.06

Table S5. Results of multivariate regression testing sexual dimorphism using RRPP. Ten log-transformed morphological traits were included as dependent variables and lineage, sex, and their interaction were included as predictor variables. Lineages included are: *occidentalis*-KL, nana4, and nana1. *P*-values < 0.05 appear in bold.

	df	SS	MS	R^2	*F*	*Z*	*P*
Lineage	2	31.861	15.9307	0.774	184.45	9.2618	**0.001**
Sex	1	0.252	0.2522	0.006	2.92	1.4784	0.073
Lineage*Sex	2	0.147	0.0737	0.003	0.85	0.1700	0.442
Residuals	103	8.896	0.0864	0.216			
Total	108	41.157					

Table S6. Dtrios results obtained vis *Dsuite*, with p-values adjusted using the False Discovery Rate method.

P1	P2	P3	D-statistic	Z-score	p-value (FDR)	f4-ratio
nana4	nana1	multiporosa	0.284584	3.06836	0.0177639	0.121482
nana1	nanamulti	multiporosa	0.0533355	0.440712	0.72783667	0.0295631
multiporosa	occiKL	nana1	0.0695736	0.483273	0.72783667	0.0531024
multiporosa	occiOR	nana1	0.0969976	0.684832	0.66425962	0.0913703
occiYI	multiporosa	nana1	0.121689	0.770486	0.6389978	0.0786361
nana4	nanamulti	multiporosa	0.282943	2.31945	0.11882733	0.147285
multiporosa	occiKL	nana4	0.106391	0.749034	0.6389978	0.0649852
multiporosa	occiOR	nana4	0.109319	0.824108	0.6389978	0.08476
occiYI	multiporosa	nana4	0.0970134	0.565673	0.71452	0.0597375
occiKL	multiporosa	nanamulti	0.145955	0.84852	0.6389978	0.054741
occiOR	multiporosa	nanamulti	0.0648351	0.411629	0.72783667	0.0292221
occiYI	multiporosa	nanamulti	0.466827	3.01881	0.0177639	0.151488
occiOR	occiKL	multiporosa	0.0343869	0.247926	0.804192	0.0194288
occiKL	multiporosa	occiYI	0.141304	0.867589	0.6389978	0.115399
occiOR	multiporosa	occiYI	0.181241	1.05799	0.6389978	0.151047
nana4	nanamulti	nana1	0.299879	3.16211	0.0177639	0.432679
nana4	nana1	occiKL	0.275991	3.30441	0.01665591	0.154725
nana4	nana1	occiOR	0.279501	3.33162	0.01665591	0.137765
nana4	nana1	occiYI	0.242256	2.02588	0.18715025	0.127256
nanamulti	nana1	occiKL	0.100711	0.916269	0.6389978	0.0617296
nanamulti	nana1	occiOR	0.0833177	0.824518	0.6389978	0.0442314
nanamulti	nana1	occiYI	0.186203	1.58605	0.35868	0.0968816
occiKL	occiOR	nana1	0.054689	0.535398	0.71493534	0.0394492
occiYI	occiKL	nana1	0.163246	1.18426	0.59078	0.133131
occiYI	occiOR	nana1	0.167869	1.25977	0.55933231	0.164391
nana4	nanamulti	occiKL	0.180278	1.49736	0.39171125	0.0987769
nana4	nanamulti	occiOR	0.207185	1.84057	0.22989575	0.0974192

nana4	nanamulti	occiYI	0.0593474	0.403954	0.72783667	0.0338986
occiKL	occiOR	nana4	0.0326519	0.321768	0.76961809	0.0213789
occiYI	occiKL	nana4	0.13687	0.928023	0.6389978	0.124962
occiYI	occiOR	nana4	0.131131	0.840268	0.6389978	0.143437
occiKL	occiOR	nanamulti	0.0946205	0.744742	0.6389978	0.0263137
occiYI	occiKL	nanamulti	0.270576	1.92666	0.21008517	0.102762
occiYI	occiOR	nanamulti	0.277177	2.06228	0.18715025	0.125966
occiOR	occiKL	occiYI	0.0781487	0.62129	0.69275241	0.0432913

Table S7. Results of the pairwise comparison of morphometric variables across the seven lineages of the *Gehyra nana-occidentalis* group. *P*-values < 0.05 appear in bold.

Lineage pairs	*d*	UCL (95%)	*Z*	*P*
multiporosa+nana1	0.671	0.368	2.641	**0.001**
multiporosa+nana4	0.358	0.333	1.719	**0.048**
multiporosa+nanamulti	0.548	0.335	2.433	**0.001**
multiporosa+occiKL	0.629	0.325	2.686	**0.001**
multiporosa+occiOR	0.515	0.575	1.414	0.105
multiporosa+occiYI	0.559	0.417	2.060	**0.014**
nana1+nana4	0.320	0.297	1.715	**0.048**
nana1+nanamulti	0.142	0.301	0.426	0.429
nana1+occiKL	1.277	0.291	4.274	**0.001**
nana1+occiOR	1.156	0.551	2.903	**0.001**
nana1+occiYI	1.214	0.393	3.541	**0.001**
nana4+nanamulti	0.197	0.252	1.185	0.166
nana4+occiKL	0.966	0.241	4.092	**0.001**
nana4+occiOR	0.847	0.526	2.422	**0.001**
nana4+occiYI	0.898	0.352	3.208	**0.001**
nanamulti+occiKL	1.161	0.248	4.371	**0.001**
nanamulti+occiOR	1.042	0.532	2.769	**0.001**
nanamulti+occiYI	1.091	0.357	3.574	**0.001**
occiKL+occiOR	0.137	0.526	-0.459	0.648
occiKL+occiYI	0.152	0.356	0.309	0.449
occiOR+occiYI	0.168	0.590	-0.331	0.646

Table S8. Trait loadings for PC axes 1–3 for the PCA of morphological traits across the seven focal lineages of the *Gehyra nana-occidentalis* group. Values that are 70% or more of the highest loading for each axis are in bold. Abbreviations are as follows: SVL, snout-to-vent length; HL, head length; HD, head depth; HW, head width; SL, snout length; OW, orbit width; WBE, width-between-eyes; ILL, interlimb length; HLL, hindlimb length; FLL, forelimb length.

Trait (log transformed)	PC1 (95%)	PC2 (1.1%)	PC3 (0.6%)
SVL	**-2.041**	0.031	-0.026
HL	**-2.039**	0.014	-0.031
HD	**-1.955**	**-0.607**	0.120
HWL	**-2.008**	-0.023	-0.149
SL	**-2.031**	0.011	-0.027
OW	**-1.994**	0.123	-0.186
WBE	**-1.983**	0.044	**-0.383**
ILL	**-2.007**	0.034	0.078
HLL	**-2.016**	0.150	**0.280**
FLL	**-2.003**	0.207	**0.321**